VEÐURSTOFA ÍSLANDS

Report
05015

Kristján Ágústsson
Páll Halldórsson

Seismic hazard in the Hengill area based on the SIL earthquake catalogue

First results

VÍ-ES-07
Reykjavík
August 2005

Contents

ABSTRACT

Maps with average recurrence time of horizontal acceleration based on the SIL catalogue from 1991 through 2000 have been made in the Hengill area and its surroundings. The dataset, which covers approximately 10 years period, is complete down to local moment magnitude 1. Comparision with similar maps based on catalogues covering 104 years and and earthquakes with local magnitude above 4 is excellent.

INTRODUCTION

The largest geothermal power plant in Iceland, Nesjavellir, is located in the northern part of the Hengill area. The plant is owned by Reykjavík Energy. Presently, Reykjavík Energy is constructing a second large power plant in the southwestern part of the Hengill area and there are plans for further exploitation of the area. The plants produce both hot water for domestic heating in the capital city of Reykjavík as well as electricity. Due to these investments and the security of the inhabitants of Reykjavík, assessment of hazard in the area is of utmost importance.

One of the goals of this investigation is to find out how reliable estimates of earthquake hazards based on the SIL catalogue are and how these estimates are compared to former estimates which are based on earthquakes of magnitude larger than 4 in the last century, some of which are not instrumental (Ambraseys and Sigbjörnsson, 2000; Halldórsson and Sveinsson 1994) The SIL system has effectively been in operation since 1991 (Böðvarsson et al., 1999). During this time over 200 thousand events have been located. Several large earthquakes have occurred (Jakobsdóttir et al., 2002; Þorbjarnardóttir et al., 2003a, 2003b), earthquakes with recurrence time of 100 years or more, which can lead to overestimation of the seismic hazard when based on this short time period.

The Hengill area is at a triple junction (Figure 1) where the Reykjanes ridge, which is the landward continuation of the mid-Atlantic ridge, the south Iceland seismic zone and the so-called western volcanic zone meet.

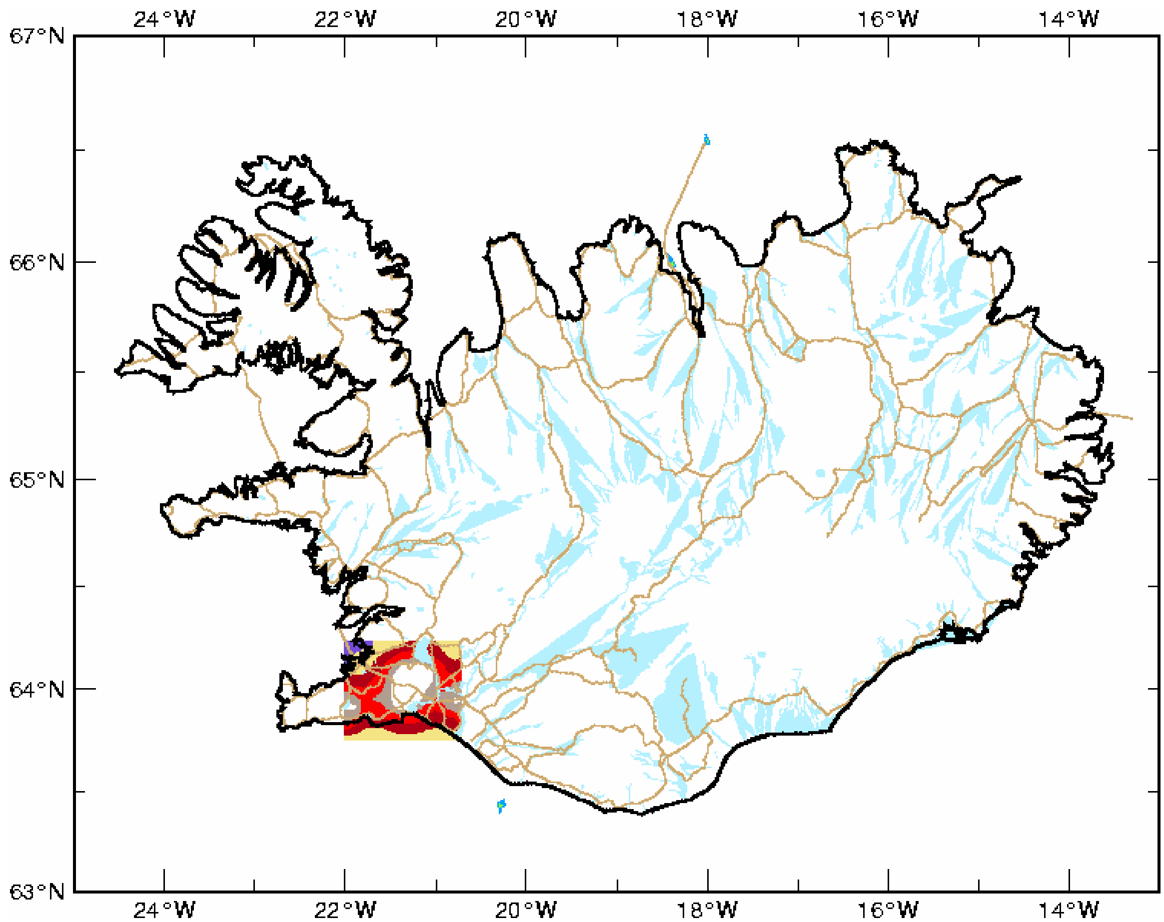

Figure 1. *The investigated area is the colored rectangle in the southwest corner of Iceland.*

During the period 1993 to 1998 seismic activity was intense in the area (Figure 2), culminating in two local magnitude 5 earthquakes, one in the summer and one in the autumn of 1998 (Vogfjörð et al., 2005a; Rögnvaldsson et al., 1998a, 1998b) Since then the area has gradually become relatively quiet.

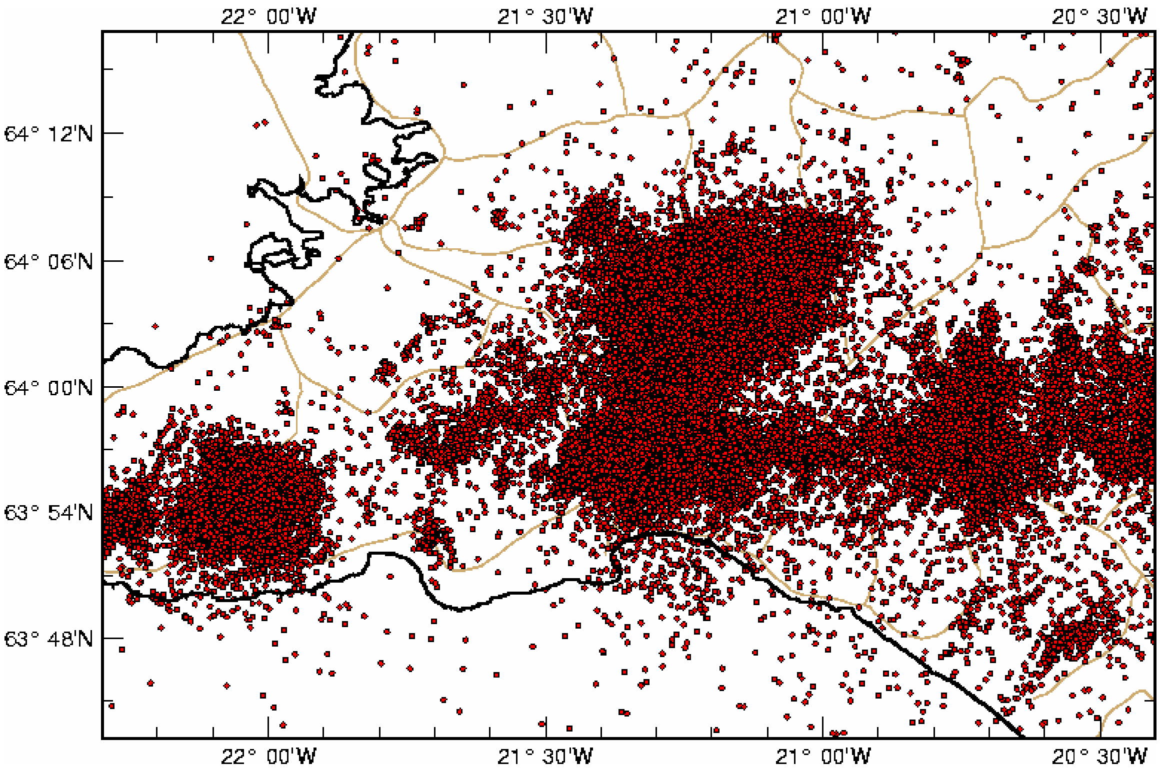

Figure 2. *Earthquakes in the Hengill area (center of the figure) and surroundings during the period from 1991 to 2000.*

Recently, two groups have presented a probilistic hazard zoning (PSHA) for Iceland (Halldórsson and Sveinsson 1994; Sólnes et al., 2004). Both groups used the same dataset but their approach was slightly different. The catlogue they used includes earthquakes from 1896 to 2000 of magnitude above 4. Most of the large earthquakes occurring after 1912 are recorded on seismometers, but information on many large earthquakes from 1896 is based on intensity observations. Sólnes et al. (2004) extended the catalogue by use of a Monte Carlo technique while the group representing the Eurocode Council used the catalogue directly. The results of the two groups are consistent with only minor differences. Mainly in that the Eurocode group obtains slightly higher accelerations in the Reykjavík area.

DATA AND DATA PROCESSING

In the analysis we calculate values on a grid with 0.04°NS and 0.1°EW mesh size. The grid extends from 63.8° to 64.2°N latitude and 20.8° to 21.9°W longitude. At each gridpoint we investigate the frequency-magnitude relation (b-value) for an area of 30 km radius around the gridpoint. Furthermore, we investigate the frequency vs. horizontal acceleration due to earthquakes within a radius of 150 km around each gridpoint. The attenuation formula used is that derived by Halldórsson and Sveinsson (2003) and all values and calulations are scaled to annual values.

The dataset used is the SIL catalogue from the middle of the year 1991 to the end of the year 2000, consisting of over 170 thousand events. In the analysis we use the local moment magnitude (M_{LW}) (Guðmundsson et al., 2005). M_{LW} and the local magnitude (M_L) correlate quite well. The moment magnitude in the Harvard CMT (M_W) catalogue is greater for the largest earthquakes in 1998 and 2000.

Using a 30 km radius, the data seems to be complete down to M_{LW} of approximately 0.5 (Appendix A) but in the b-value estimate, only M_{LW} above 1 are used. M_{LW} of the largest earthquakes are underestimated. Furthermore M_{LW} of several earthquakes in the interval between approximately 3.5 and 5.5 are not certain, partly due to the fact that several earthquakes in this size interval are superimposed on the waveforms of larger preceding events, and determination of their characteristics is in some cases a delicate manual process. In this dataset a rough estimate of their magnitudes is based on amplitude comparations and in some cases the M_L is used. Uncertainty in these magnitude determinations or some systematic error may be the reason for the deviations of the cumulative curve from a line (Appendix A).

Horizontal acceleration is calculated according to

$$\log(a) = 0.484m - 1.5989*\log(R) - 2.1640 + 0.3091*n$$

where a is horizontal acceleration as a fraction of the acceleration of gravity (g), m is magnitude, in this case the M_{LW} (Halldórsson and Sveinsson, 2003). R is distance. n is the number of standard deviatons and in our calculations it is equal to 0. The formula is not valid within the source area of the earthquakes. Acceleration from earthquakes within a 150 km radius of each gridpoint was calculated. On a cumulative curve of log(N) vs. log(a) (Appendix B), a rather clear relation exists for log(a) greater than -3 (0.1% of g). From the relation we calculate the accelerations expected to be reached or exceeded for different time periods. The the calculations are done for periods of 100, 475, 2500 and 10000 years (Appendix C).

No declustering attempt is made. The charateristics of earthquake clusters or swarms in this statistical sense has not been investigated for the SIL catalogue. In the Hengill area, the activity has been more or less continuous with temporary more intense activity in the whole area but not restricted to typical fore- and/or aftershock sequences on definite faults. In the year 2000 it is obvious that static stress changes associated with the June 17 earthquake triggered the June 21 earthquake (Árnadóttir et al., 2003). Dynamic stress changes (surface waves) associated with the same earthquake also triggered earthquakes (Antonioli et al., 2005; Vogfjörð et al., 2005b). During the 5 years since these events, a continuous activity has been observed on all the faults that were active at that time. Therefore in a strict sense almost all seismic activity in south Iceland, at least since 2000, is a single cluster. The step from this extreme interpretation to other extreme, i.e. all events are independent, which we have taken in this preliminary investigation, may be disputable. But in the end the definition of dependence is subjective.

RESULTS

The b-values are rather constant in the Hengill area and in the western part of the south Iceland seismic zone (Figure 3) with values around 0.87. They decrease systematically towards west and southwest, reaching a value of about 0.8 at the border of our network, as the seismicity decreases (Figure 3).

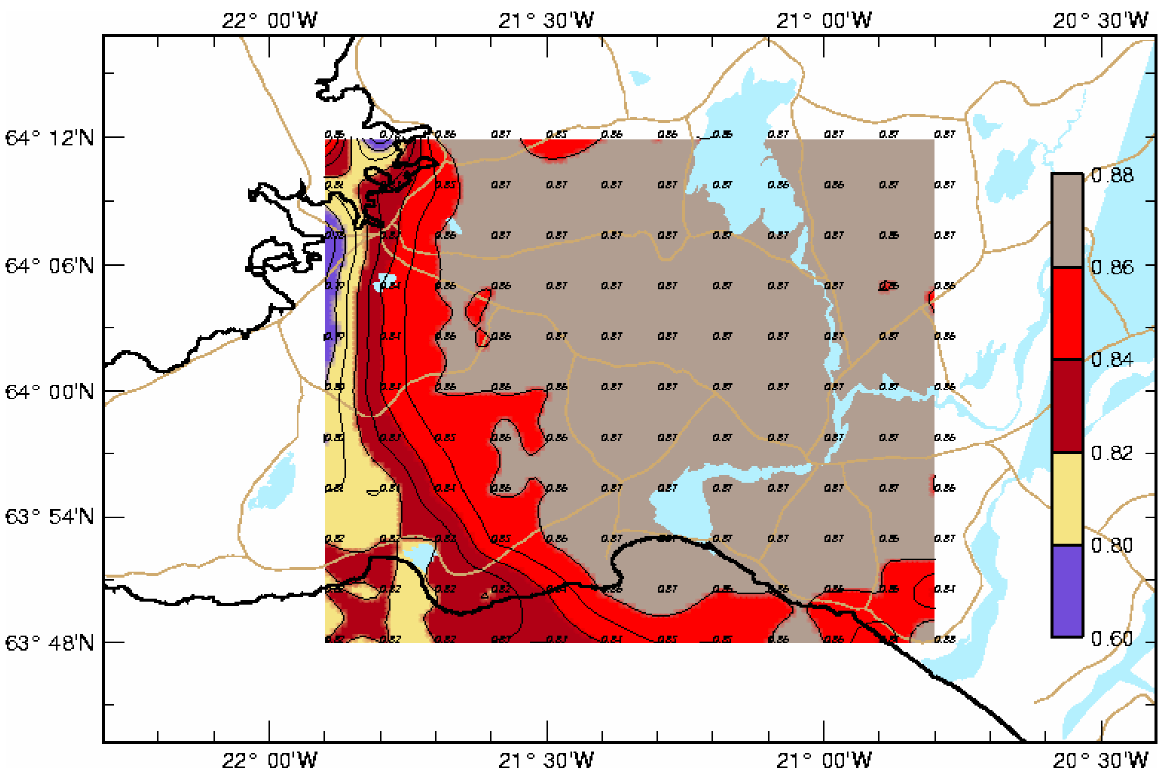

Figure 3. *Calculated yearly b-values in a circular area of 30 km radius around the corresponding gridpoint.*

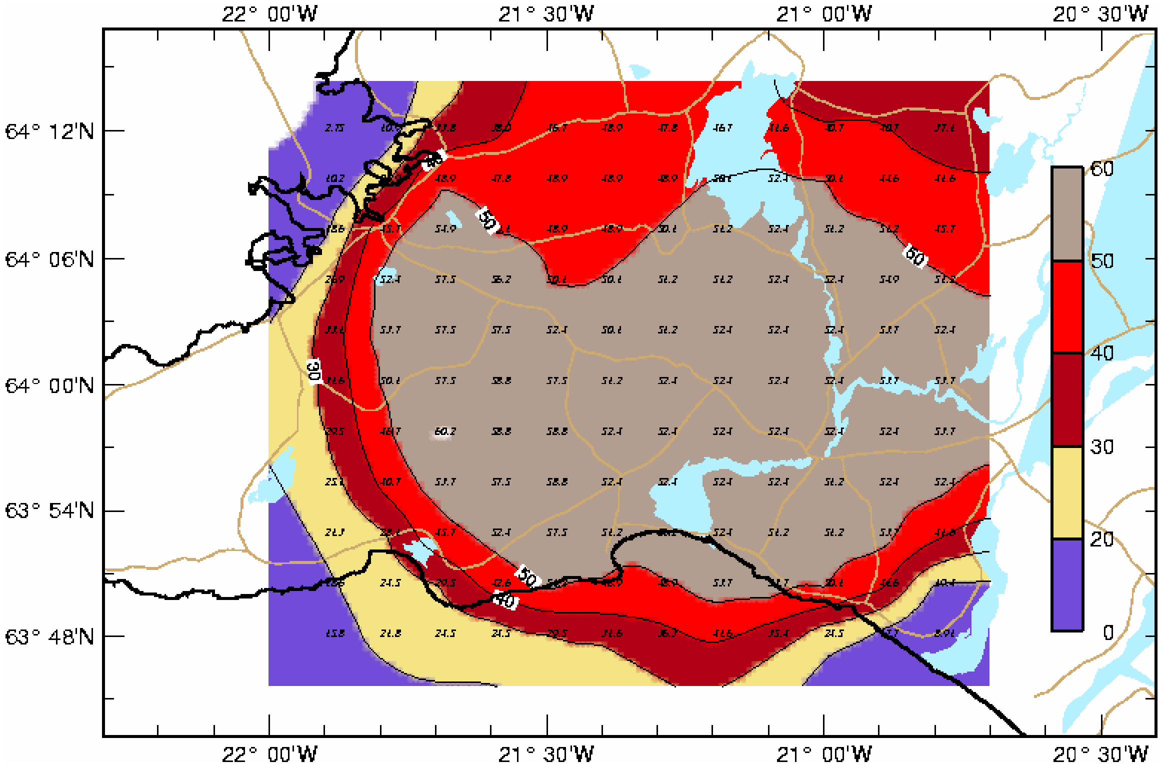

Figure 4. *Number of earthquakes per year with M_{LW} of 3 and more in a circular area of 30 km radius around the corresponding gridpoint.*

In Figure 4, the annual number of earthquakes with magnitude above 3, within a radius of 30 km from each gridpoint is shown. In the central part of the area we have more than 50 earthquakes of this size within 30 km distance. The number decreases towards the borders of the network, particularly towards west where the number of events is about or less than 20.

Hazard maps are made for four different average recurrence times (Appendix C). The standard map (Figure 5) shows the 475 years average recurrence time corresponding to 10% probability that the acceleration will reach or exceed the value within the next 50 years. Acceleration values in the areas with the highest values are not reliable (white areas on Figure 5 and on figures in Appendix C), particularly when the recurrence time is short. That is due to the fact that the attenuation formula is not valid in the vicinity of the source.

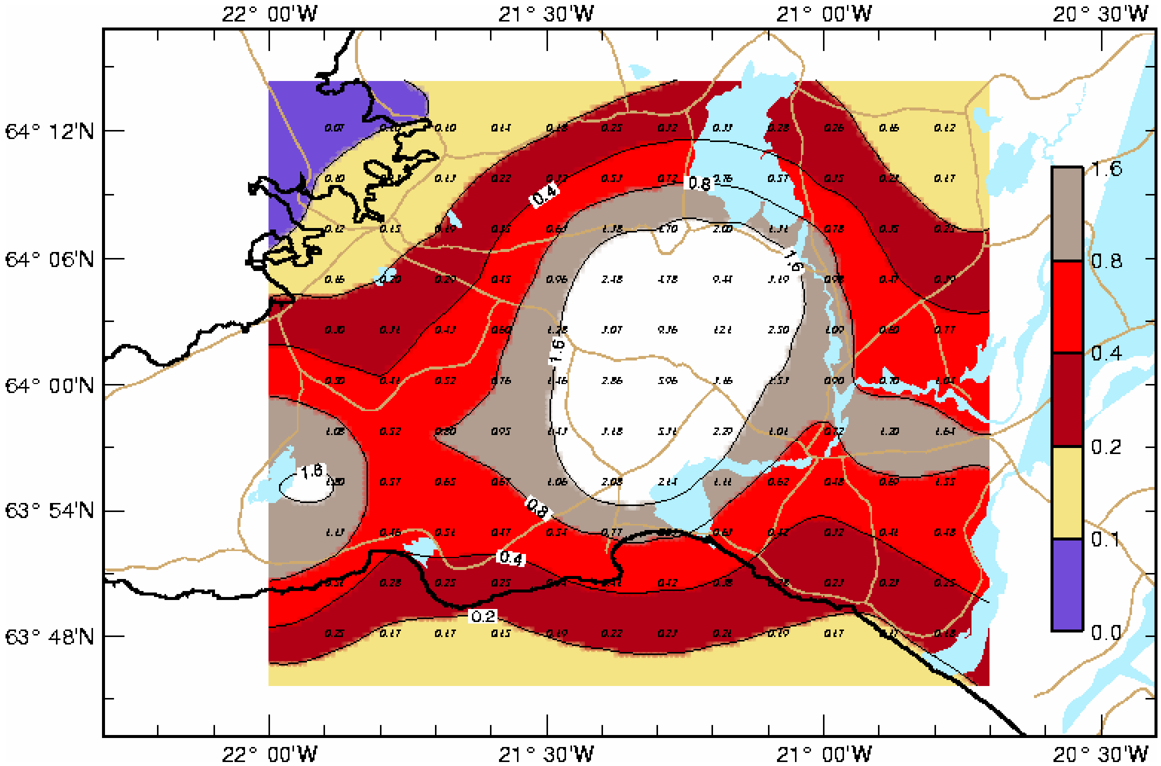

Figure 5. *Seismic hazard map of the Hengill area, Iceland, showing acceleration expected to be reached or exceeded in a period of 475 years. The Figure shows the 475 years average recurrence time corresponding to 10% probability that the acceleration will reach or exceed the value within the next 50 years.*

CONCLUSIONS

The preliminary result of using the SIL catalogue to calculate seismic hazard maps is promising. The result for the investigated area is comparable to former studies. Care has to be taken regarding bias due to the large events that have occurred during this period and similarly seismic gaps, e.g. possibly at the western boundary of our grid. Further, analysis on the effect of clustering needs to be done.

The SIL system has much higher sensitivity than other seismic networks in Iceland. That fact and the possibility of estimating accelerations in different frequency bands makes it possible to make more detailed seismic hazard maps for Iceland, in particular for the Hengill area and the south Iceland seismic zone.

ACKNOWLEDGEMENTS

This work was funded by the European Commission and the Icelandic Meteorological Office under the project RETINA (EVG1-CT-2001-00046).
The figures were made by using the GMT public domain software (Wessel and Smith, 1998).

REFERENCES

Ambraseys, N.N. and R. Sigbjörnsson, 2000. Re-appraisal of the seismicity of Iceland. *Polytechnica - Engineering Seismology* 3, Earthquake Engineering Research Centre, University of Iceland, 96 pp.

Bergþóra S. Þorbjarnardóttir, Gunnar B. Guðmundsson and Steinunn S. Jakobsdóttir. 2003a. Seismicity in Iceland during 2001. *Jökull* (The Icelandic Journal of Earth Sciences) 52, 55-60.

Bergþóra S. Þorbjarnardóttir and Gunnar B. Guðmundsson. 2003b. Seismicity in Iceland 2002. *Jökull* (The Icelandic Journal of Earth Sciences) 53, 49-54.

Gunnar B. Guðmundsson, Kristín S. Vogfjörð and Bergþóra S. Þorbjarnardóttir. 2005. Data Status Report published in the PREPARED Third Periodic Report, February 1 - July 31, 2005. *Veðurstofa Íslands – Greinargerð.*

Júlíus Sólnes, Ragnar Sigbjörnsson and Jónas Elíasson. 2004. Probabilistic seismic hazard mapping of Iceland. Proposed seismic zoning and de-aggregation mapping for EUROCODE 8. Paper No. 2337. 13th World Conference on Earthquake Engineering, Vancouver, B.C., Canada. August 1-6, 2004.

Kristín S. Vogfjörð, Sigurlaug Hjaltadóttir and Ragnar Slunga. 2005a. Volcano-tectonic interaction in the Hengill region, Iceland, during 1993-1998. Geophysical Research Abstracts, vol. 7, 09947, EGU General Assembly, Vienna, Austria, April 24-29, 2005.

Kristín S. Vogfjörð, Sigurlaug Hjaltadóttir and Ragnar Slunga. 2005b. The M~5 triggered events in the South Iceland Seismic Zone on June 17, 2000: Determination of fault plane, magnitude and mechanism. Geophysical Research Abstracts, vol. 7, 10274, EGU General Assembly, Vienna, Austria, April 24-29, 2005.

Páll Halldórsson and Björn Ingi Sveinsson. 1994. Hröðunarkort. Í: Þjóðarskjal með FS ENV 1998-1-1:1994.

Páll Halldórsson and Björn Ingi Sveinsson. 2003. Dvínun hröðunar á Íslandi (The attenuation of acceleration in Iceland). *Veðurstofa Íslands - Greinargerð* 03025, 11 pp.

Reynir Böðvarsson, Sigurður Th. Rögnvaldsson, Ragnar Slunga and Einar Kjartansson. 1999. The SIL data acquisition system - at present and beyond year 2000. *Physics of the Earth and Planetary Interior*, 113, 89-101.

Sigurður Th. Rögnvaldsson, Gunnar B. Guðmundsson, Kristján Ágústsson, Steinunn S. Jakobsdóttir, Ragnar Slunga and Ragnar Stefánsson. 1998a. Overview of the 1993-1996 seismicity near Hengill. *Rit Veðurstofu Íslands* VÍ-R98006, 16 pp.

Sigurður Th. Rögnvaldsson, Þóra Árnadóttir, Kristján Ágústsson, Þórunn Skaftadóttir, Gunnar B. Guðmundsson, Grímur Björnsson, Kristín Vogfjörð, Ragnar Stefánsson, Reynir Böðvarsson, Ragnar Slunga Steinunn S. Jakobsdóttir, Bergþóra S. Þorbjarnardóttir, Pálmi Erlendsson, Bergur H. Bergsson, Sturla Ragnarsson, Páll Halldórsson, Barði Þorkelsson and Margrét Ásgeirsdóttir. 1998b. Skjálftahrina í Ölfusi í nóvember 1998 (An earthquake swarm in Ölfus area in November 1998). *Veðurstofa Íslands - Greinargerð* VÍ-G98046, 19 pp.

Steinunn S. Jakobsdóttir, Gunnar B. Guðmundsson and Ragnar Stefánsson. 2002. Seismicity in Iceland 1991-2000 monitored by the SIL seismic system. *Jökull* (The Icelandic Journal of Earth Sciences) 51, 87-94.

Thóra Árnadóttir, Sigurjón Jónsson, Rikke Pedersen and Gunnar B. Guðmundsson. 2003. Coulomb stress changes in the South Iceland Seismic Zone due to two large earthquakes in June 2000. *Geophysical Research Letters* 30(5).

Wessel, P. and W.H.F. Smith, 1998. New, improved version of Generic Mapping Tools Released. *Eos, Trans. AGU* 79, 579.

APPENDICES

Appendix A

The figures show the yearly cumulative number-magnitude distribution in a circular area with 30 km radius around the coordinates which are shown in the upper right corner of each figure. The number of earthquakes in the area is shown below the coordinates. The relation

$$\log(N) = a - b*m$$

where N is the number and m is the local moment magnitude is shown in the lower left corner.

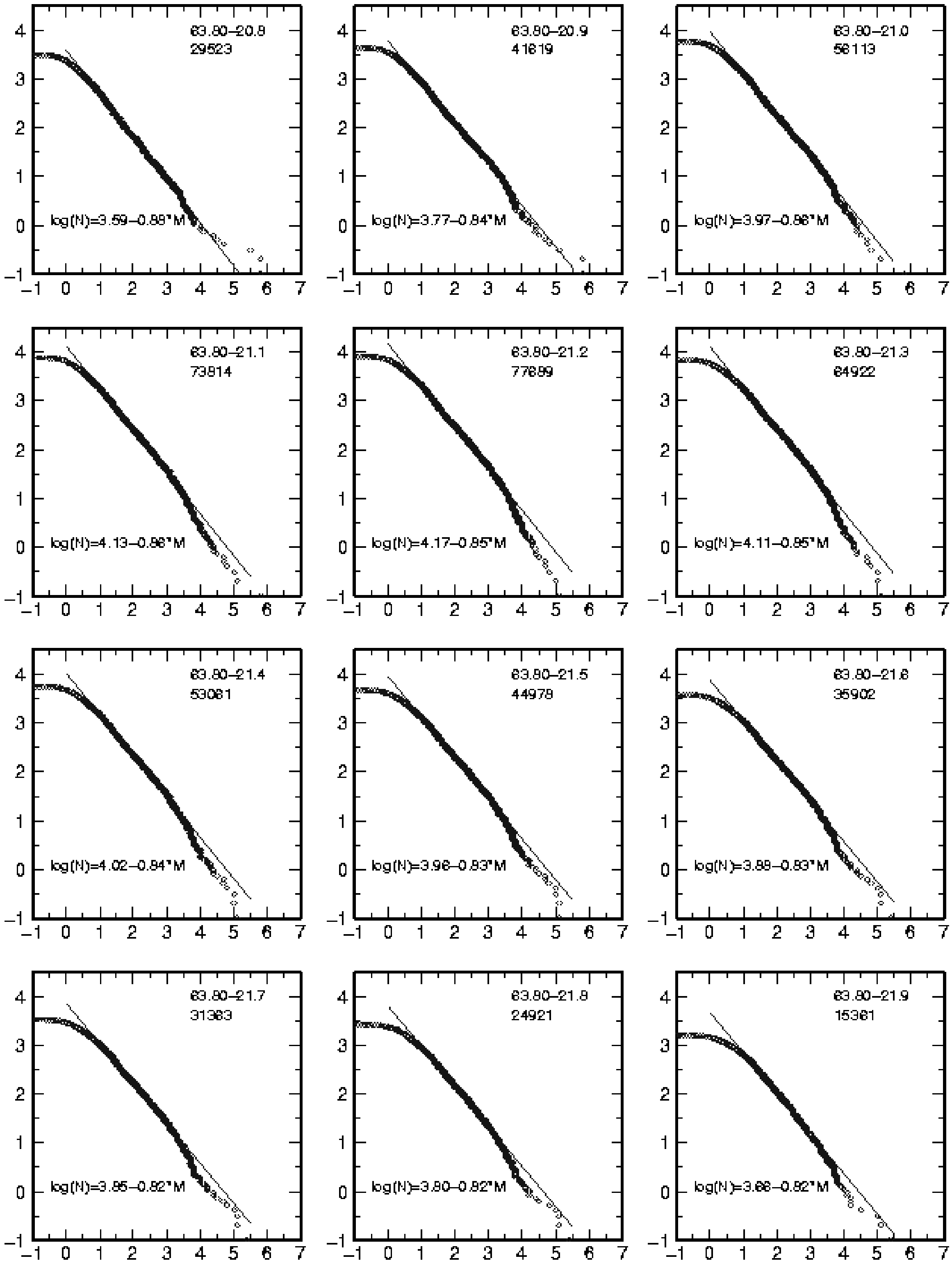
63.80–20.8
29523
log(N)=3.59–0.88*M
63.80–20.9
41619
log(N)=3.77–0.84*M
63.80–21.0
56113
log(N)=3.97–0.86*M
63.80–21.1
73814
log(N)=4.13–0.86*M
63.80–21.2
77699
log(N)=4.17–0.85*M
63.80–21.3
64922
log(N)=4.11–0.85*M
63.80–21.4
53061
log(N)=4.02–0.84*M
63.80–21.5
44978
log(N)=3.96–0.83*M
63.80–21.6
35902
log(N)=3.88–0.83*M
63.80–21.7
31363
log(N)=3.85–0.82*M
63.80–21.8
24921
log(N)=3.80–0.82*M
63.80–21.9
15361
log(N)=3.68–0.82*M

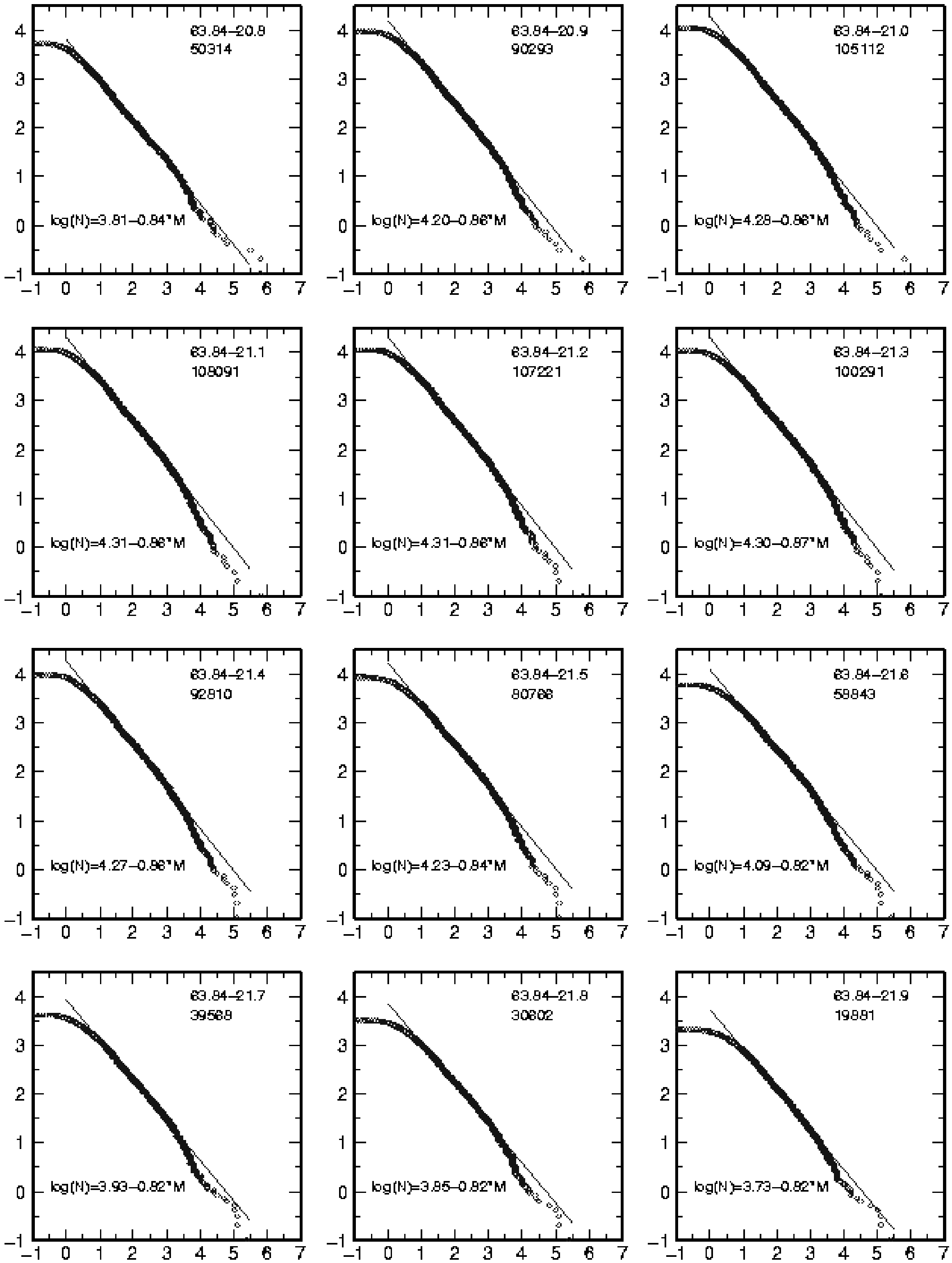
63.84–20.8
50314
log(N)=3.81–0.84*M
63.84–20.9
90293
log(N)=4.20–0.86*M
63.84–21.0
105112
log(N)=4.28–0.86*M
63.84–21.1
108091
log(N)=4.31–0.86*M
63.84–21.2
107221
log(N)=4.31–0.86*M
63.84–21.3
100291
log(N)=4.30–0.87*M
63.84–21.4
92810
log(N)=4.27–0.86*M
63.84–21.5
80768
log(N)=4.23–0.84*M
63.84–21.6
58843
log(N)=4.09–0.82*M
63.84–21.7
39588
log(N)=3.93–0.82*M
63.84–21.8
30802
log(N)=3.85–0.82*M
63.84–21.9
19881
log(N)=3.73–0.82*M

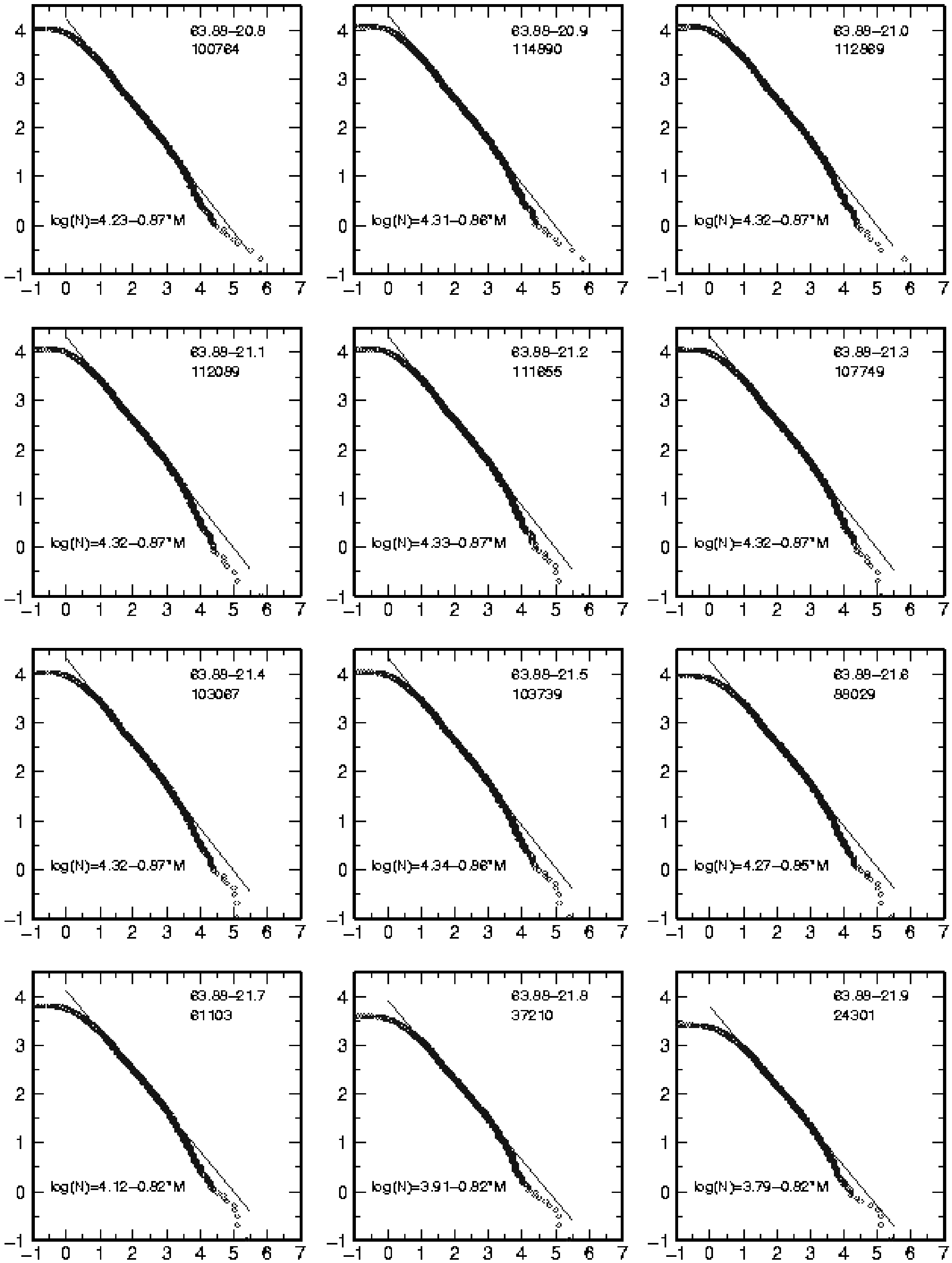
63.88–20.8
100764
log(N)=4.23–0.87*M
63.88–20.9
114890
log(N)=4.31–0.86*M
63.88–21.0
112889
log(N)=4.32–0.87*M
63.88–21.1
112089
log(N)=4.32–0.87*M
63.88–21.2
111655
log(N)=4.33–0.87*M
63.88–21.3
107749
log(N)=4.32–0.87*M
63.88–21.4
103067
log(N)=4.32–0.87*M
63.88–21.5
103739
log(N)=4.34–0.86*M
63.88–21.6
88029
log(N)=4.27–0.85*M
63.88–21.7
61103
log(N)=4.12–0.82*M
63.88–21.8
37210
log(N)=3.91–0.82*M
63.88–21.9
24301
log(N)=3.79–0.82*M

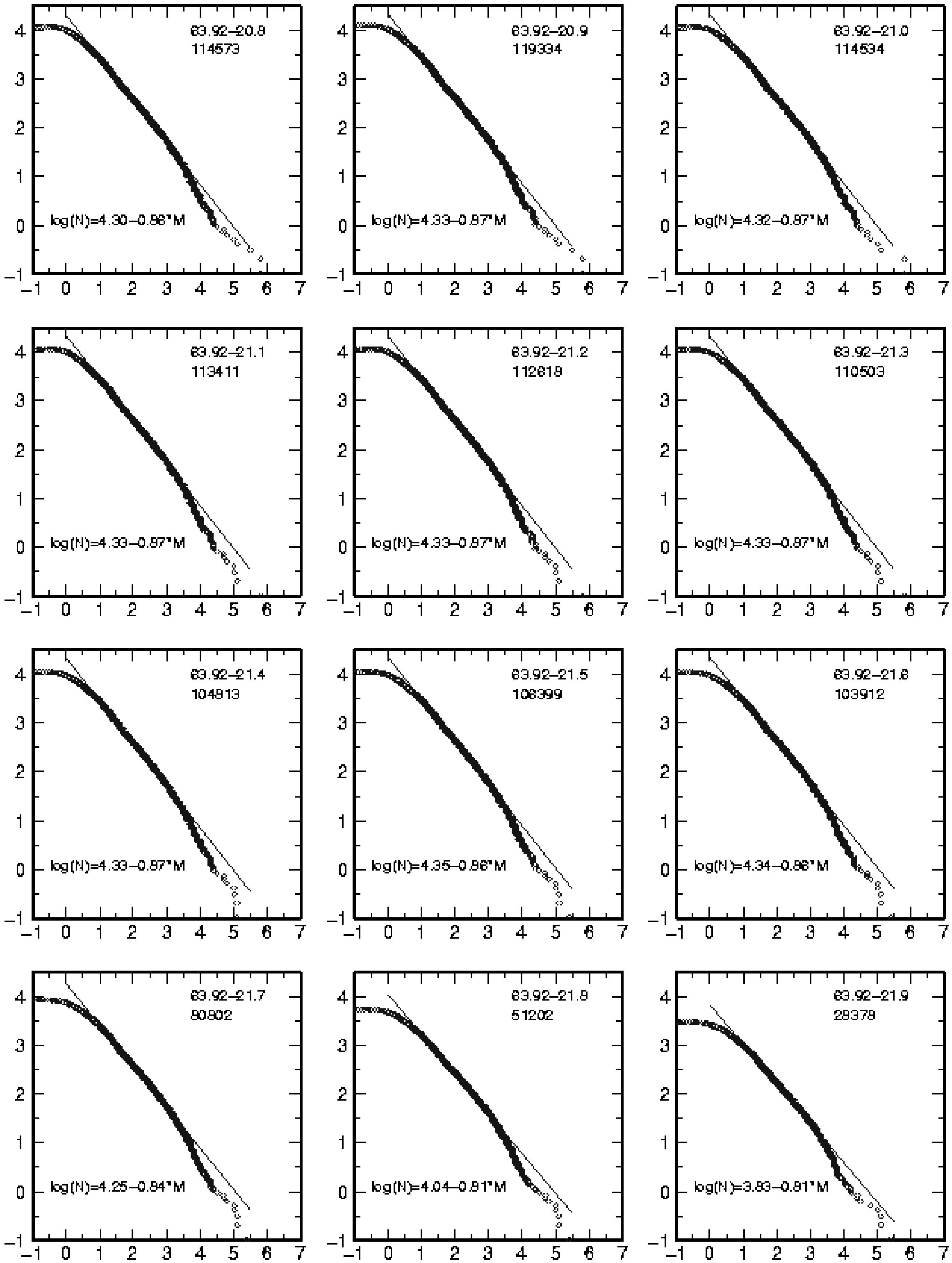
63.92−20.8
114573
log(N)=4.30−0.86*M
63.92−20.9
119334
log(N)=4.33−0.87*M
63.92−21.0
114534
log(N)=4.32−0.87*M
63.92−21.1
113411
log(N)=4.33−0.87*M
63.92−21.2
112818
log(N)=4.33−0.87*M
63.92−21.3
110503
log(N)=4.33−0.87*M
63.92−21.4
104813
log(N)=4.33−0.87*M
63.92−21.5
108399
log(N)=4.35−0.86*M
63.92−21.6
103912
log(N)=4.34−0.86*M
63.92−21.7
80802
log(N)=4.25−0.84*M
63.92−21.8
51202
log(N)=4.04−0.81*M
63.92−21.9
28378
log(N)=3.83−0.81*M

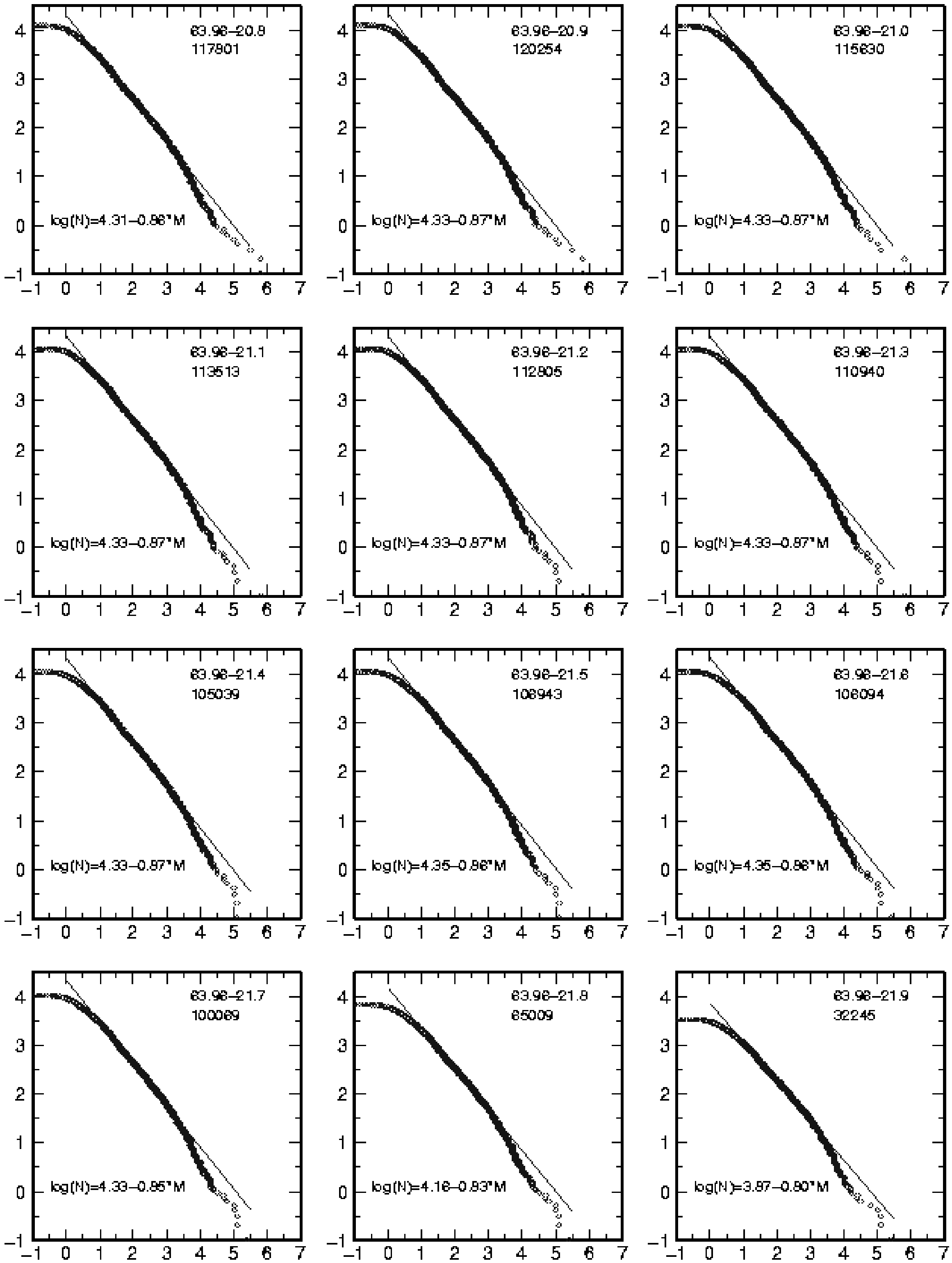
63.98–20.8
117801
log(N)=4.31–0.86*M
63.98–20.9
120254
log(N)=4.33–0.87*M
63.98–21.0
115630
log(N)=4.33–0.87*M
63.98–21.1
113513
log(N)=4.33–0.87*M
63.98–21.2
112805
log(N)=4.33–0.87*M
63.98–21.3
110940
log(N)=4.33–0.87*M
63.98–21.4
105039
log(N)=4.33–0.87*M
63.98–21.5
108943
log(N)=4.35–0.86*M
63.98–21.6
106094
log(N)=4.35–0.86*M
63.98–21.7
100069
log(N)=4.33–0.85*M
63.98–21.8
65009
log(N)=4.16–0.83*M
63.98–21.9
32245
log(N)=3.87–0.80*M

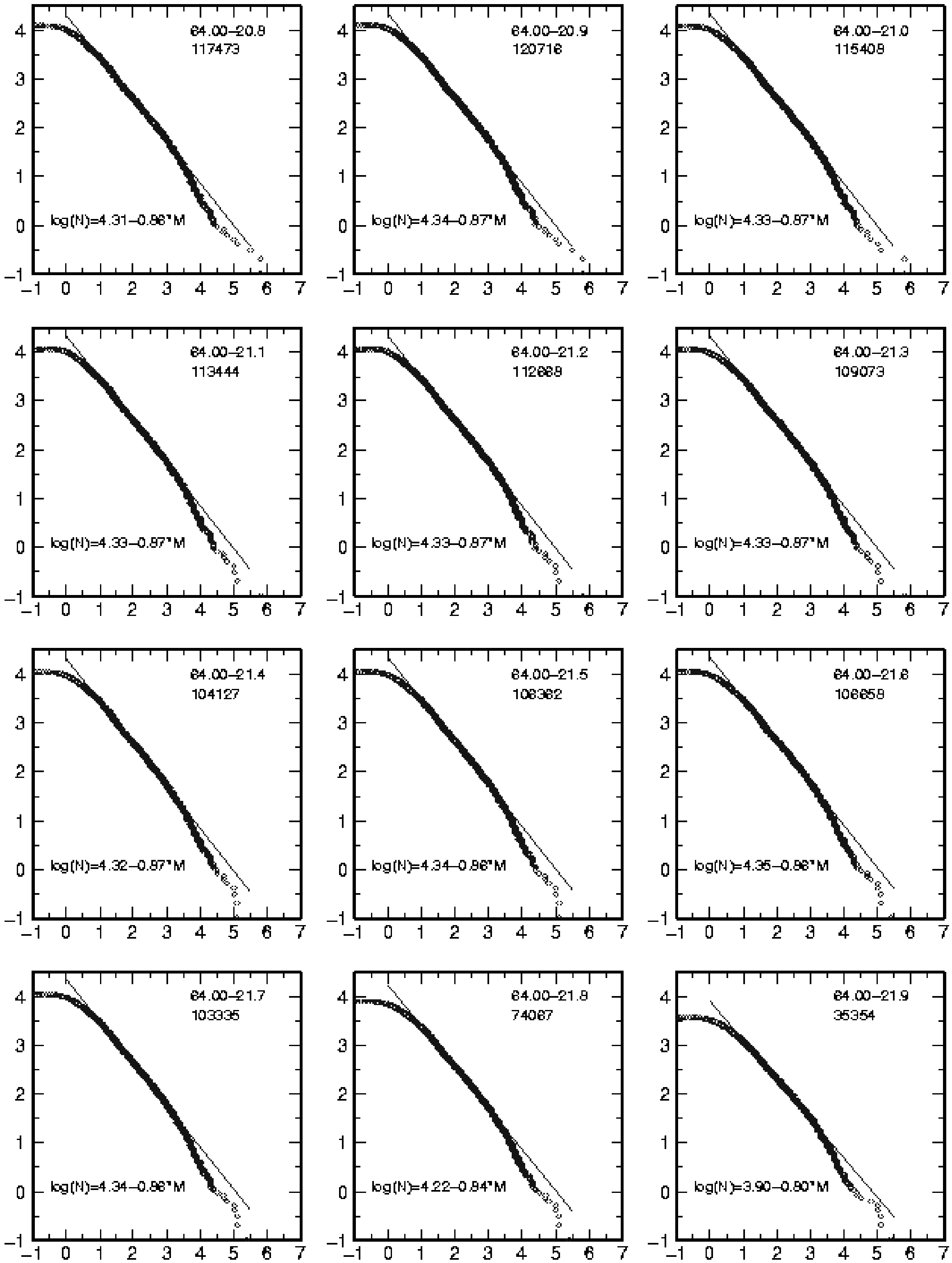

64.00–20.8
117473
log(N)=4.31–0.86*M
64.00–20.9
120716
log(N)=4.34–0.87*M
64.00–21.0
115408
log(N)=4.33–0.87*M
64.00–21.1
113444
log(N)=4.33–0.87*M
64.00–21.2
112688
log(N)=4.33–0.87*M
64.00–21.3
109073
log(N)=4.33–0.87*M
64.00–21.4
104127
log(N)=4.32–0.87*M
64.00–21.5
108382
log(N)=4.34–0.86*M
64.00–21.6
106858
log(N)=4.35–0.86*M
64.00–21.7
103335
log(N)=4.34–0.86*M
64.00–21.8
74067
log(N)=4.22–0.84*M
64.00–21.9
35354
log(N)=3.90–0.80*M

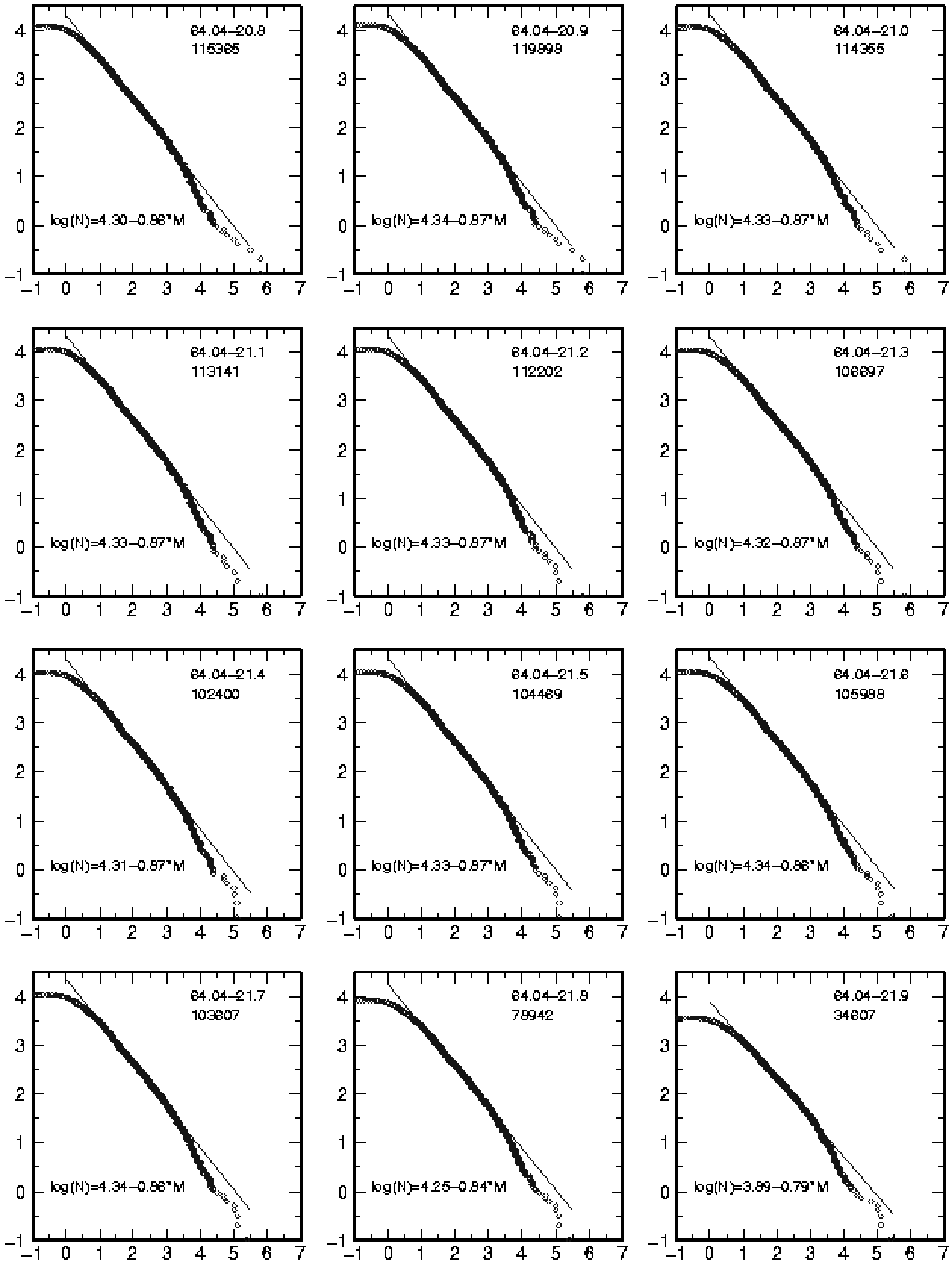
64.04−20.8
115365
log(N)=4.30−0.86*M
64.04−20.9
119898
log(N)=4.34−0.87*M
64.04−21.0
114355
log(N)=4.33−0.87*M
64.04−21.1
113141
log(N)=4.33−0.87*M
64.04−21.2
112202
log(N)=4.33−0.87*M
64.04−21.3
106697
log(N)=4.32−0.87*M
64.04−21.4
102400
log(N)=4.31−0.87*M
64.04−21.5
104469
log(N)=4.33−0.87*M
64.04−21.6
105988
log(N)=4.34−0.86*M
64.04−21.7
103607
log(N)=4.34−0.86*M
64.04−21.8
78942
log(N)=4.25−0.84*M
64.04−21.9
34607
log(N)=3.89−0.79*M

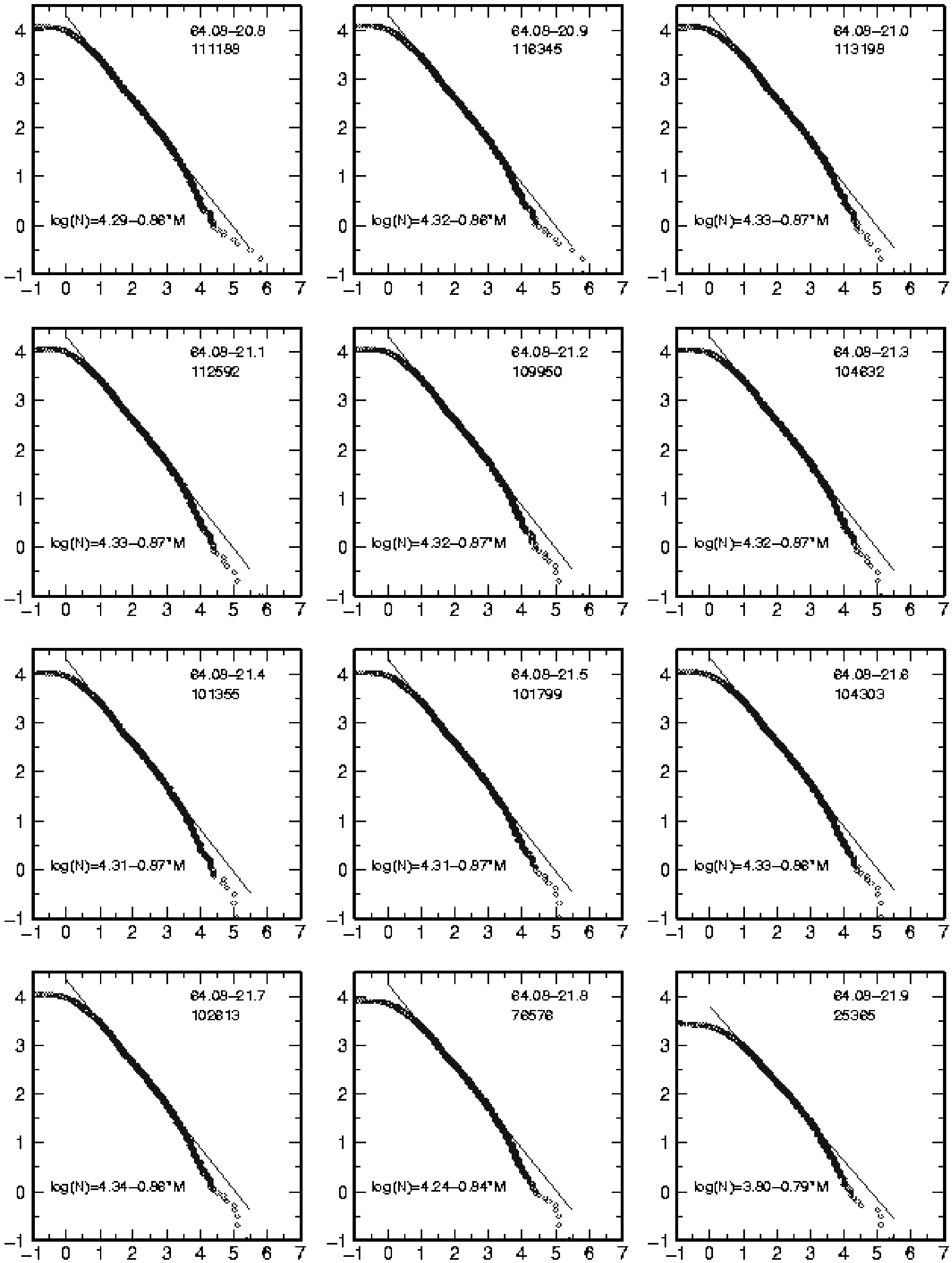
64.08−20.8
111189
log(N)=4.29−0.86*M
64.08−20.9
118345
log(N)=4.32−0.86*M
64.08−21.0
113198
log(N)=4.33−0.87*M
64.08−21.1
112592
log(N)=4.33−0.87*M
64.08−21.2
109950
log(N)=4.32−0.87*M
64.08−21.3
104632
log(N)=4.32−0.87*M
64.08−21.4
101355
log(N)=4.31−0.87*M
64.08−21.5
101799
log(N)=4.31−0.87*M
64.08−21.6
104303
log(N)=4.33−0.86*M
64.08−21.7
102813
log(N)=4.34−0.86*M
64.08−21.8
76576
log(N)=4.24−0.84*M
64.08−21.9
25365
log(N)=3.80−0.79*M

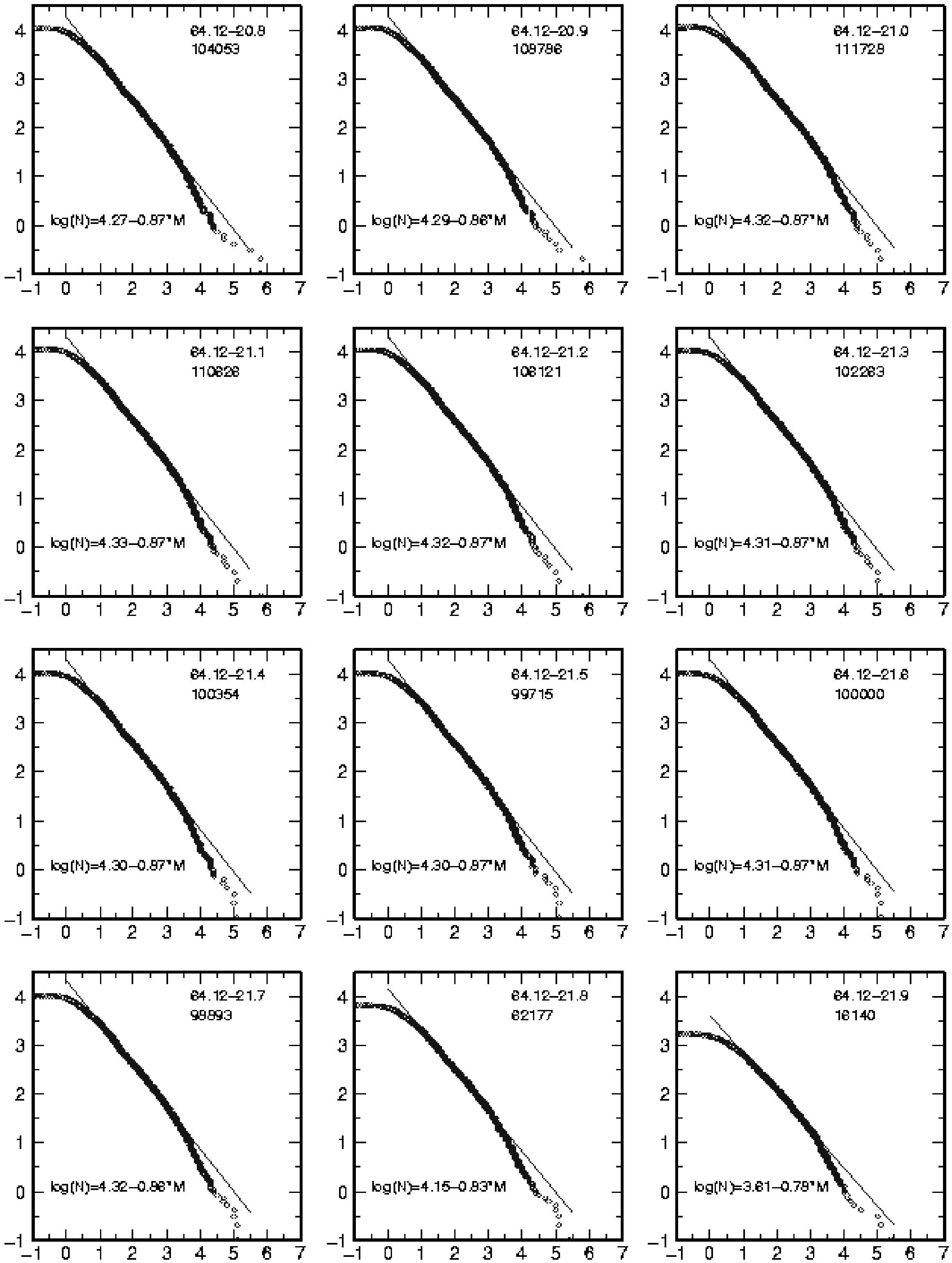
64.12−20.8
104053
log(N)=4.27−0.87*M
64.12−20.9
109786
log(N)=4.29−0.86*M
64.12−21.0
111728
log(N)=4.32−0.87*M
64.12−21.1
110828
log(N)=4.33−0.87*M
64.12−21.2
108121
log(N)=4.32−0.87*M
64.12−21.3
102283
log(N)=4.31−0.87*M
64.12−21.4
100354
log(N)=4.30−0.87*M
64.12−21.5
99715
log(N)=4.30−0.87*M
64.12−21.6
100000
log(N)=4.31−0.87*M
64.12−21.7
98893
log(N)=4.32−0.86*M
64.12−21.8
62177
log(N)=4.15−0.83*M
64.12−21.9
16140
log(N)=3.61−0.78*M

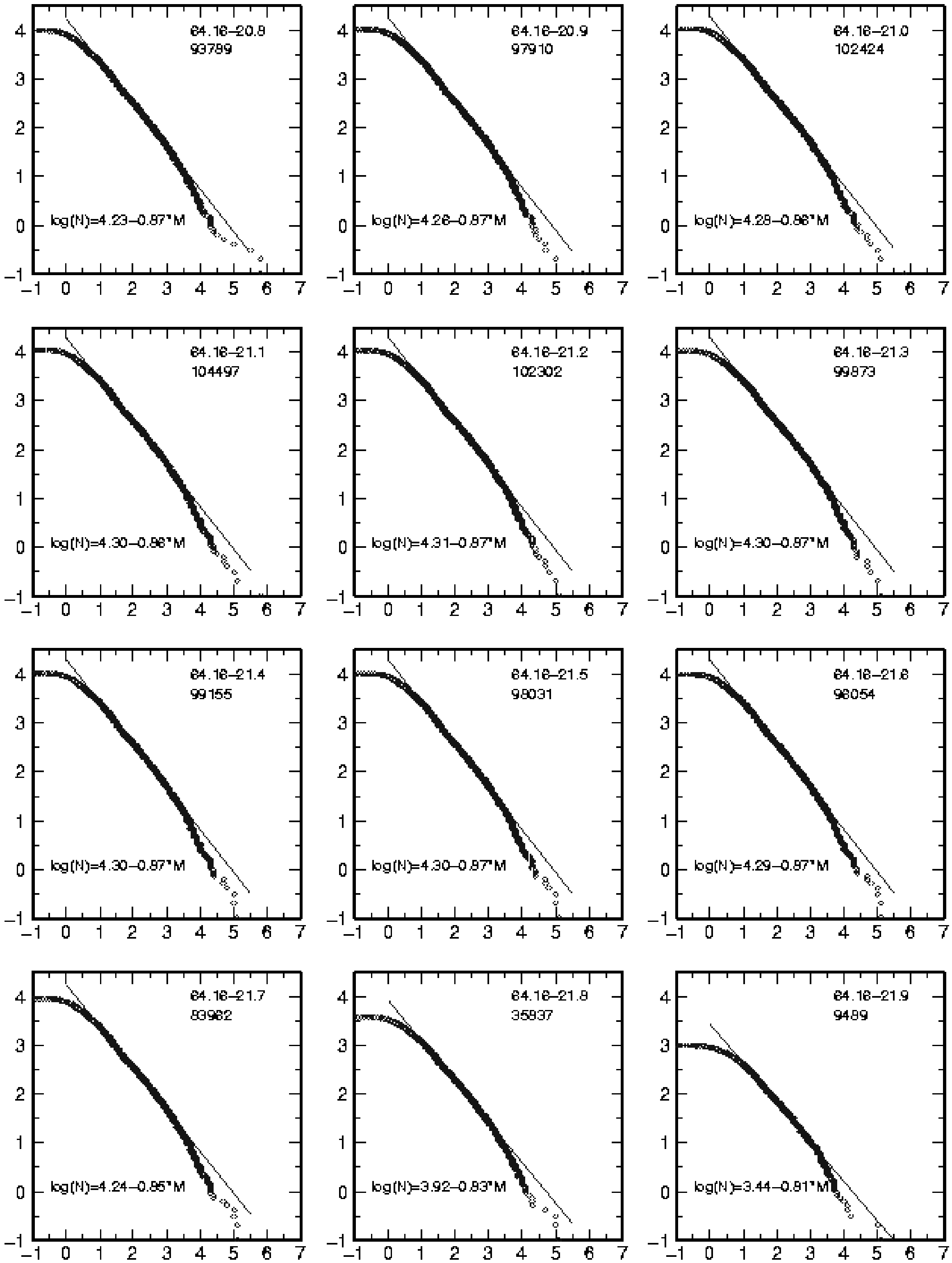
64.16–20.8
93789
log(N)=4.23–0.87*M
64.16–20.9
97910
log(N)=4.26–0.87*M
64.16–21.0
102424
log(N)=4.28–0.86*M
64.16–21.1
104497
log(N)=4.30–0.86*M
64.16–21.2
102302
log(N)=4.31–0.87*M
64.16–21.3
99873
log(N)=4.30–0.87*M
64.16–21.4
99155
log(N)=4.30–0.87*M
64.16–21.5
98031
log(N)=4.30–0.87*M
64.16–21.6
96054
log(N)=4.29–0.87*M
64.16–21.7
83962
log(N)=4.24–0.85*M
64.16–21.8
35837
log(N)=3.92–0.83*M
64.16–21.9
9489
log(N)=3.44–0.81*M

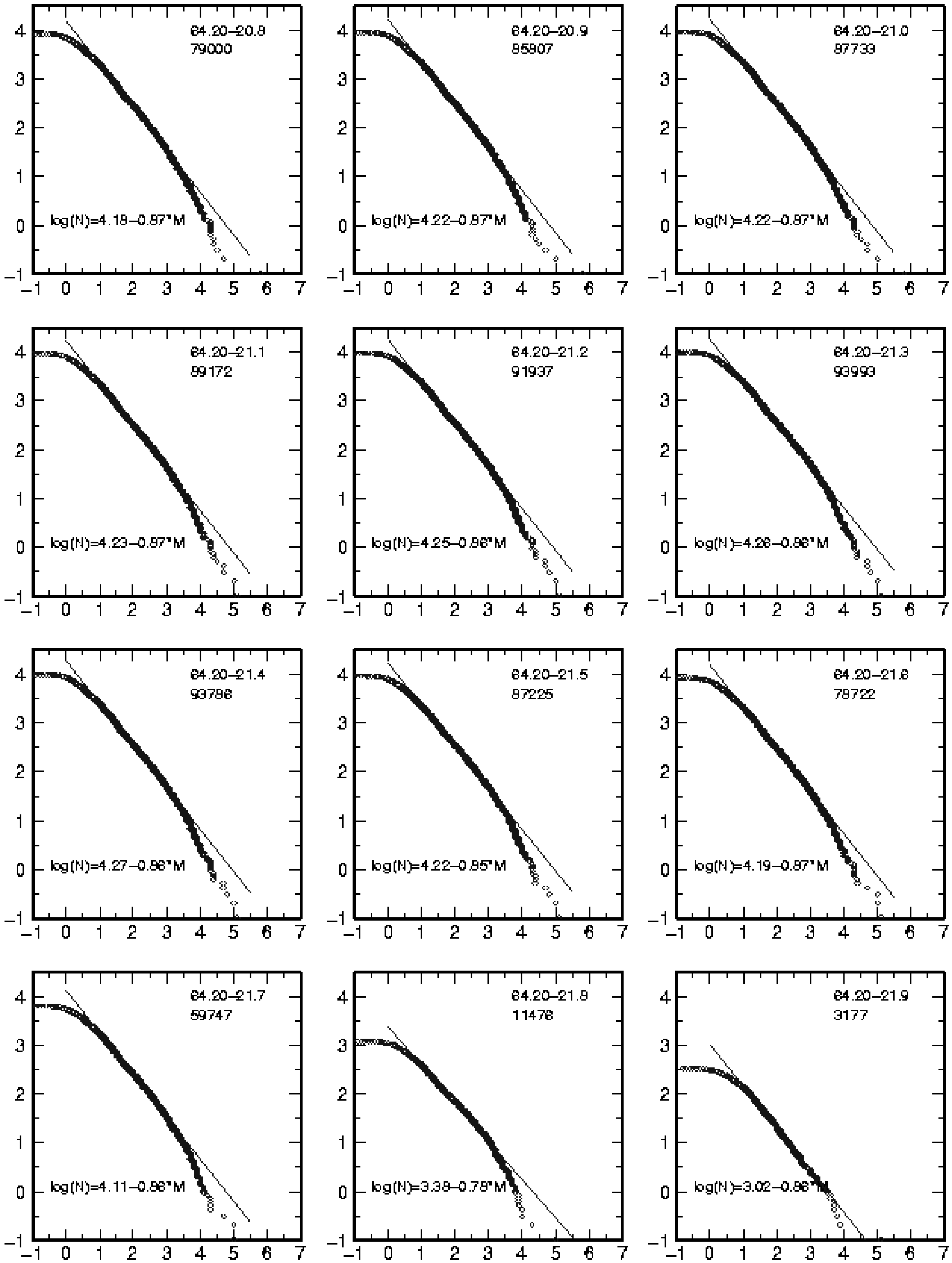

64.20−20.8
79000
log(N)=4.18−0.87*M
64.20−20.9
85807
log(N)=4.22−0.87*M
64.20−21.0
87733
log(N)=4.22−0.87*M
64.20−21.1
89172
log(N)=4.23−0.87*M
64.20−21.2
91937
log(N)=4.25−0.86*M
64.20−21.3
93993
log(N)=4.26−0.86*M
64.20−21.4
93786
log(N)=4.27−0.86*M
64.20−21.5
87225
log(N)=4.22−0.85*M
64.20−21.6
78722
log(N)=4.19−0.87*M
64.20−21.7
59747
log(N)=4.11−0.86*M
64.20−21.8
11476
log(N)=3.38−0.78*M
64.20−21.9
3177
log(N)=3.02−0.86*M

Appendix B

The figures show the yearly cumulative number-acceleration distribution in a circular area with 150 km radius around the coordinates which are shown in the upper right corner of each figure. The number of earthquakes used in the plot is shown below the coordinates. The relation

$$\log(N) = a - b*\log(a)$$

where N is the number and a is the acceleration is shown in the lower left corner.

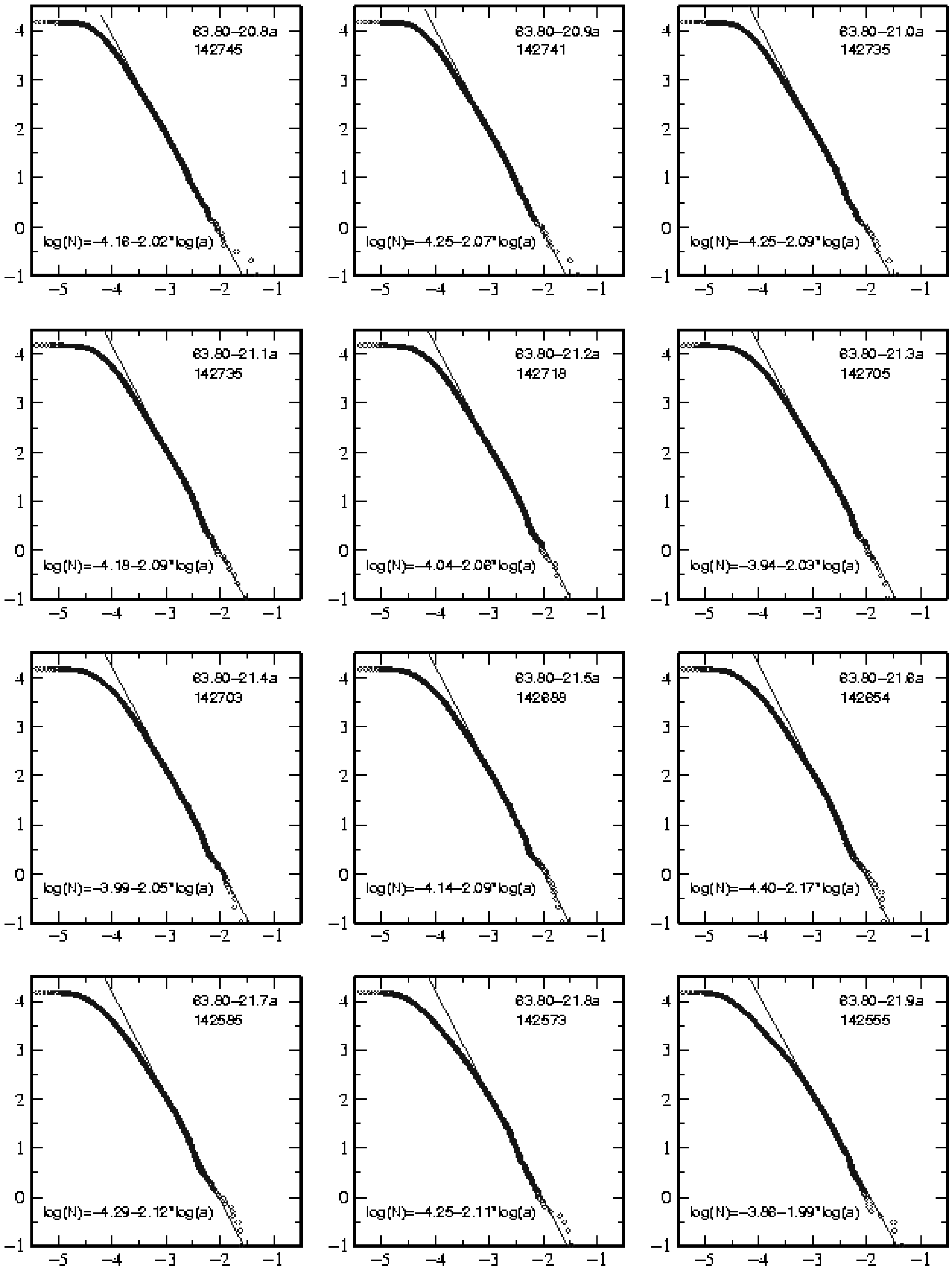

63.80−20.8a
142745
log(N)=−4.16−2.02*log(a)
63.80−20.9a
142741
log(N)=−4.25−2.07*log(a)
63.80−21.0a
142735
log(N)=−4.25−2.09*log(a)
63.80−21.1a
142735
log(N)=−4.18−2.09*log(a)
63.80−21.2a
142718
log(N)=−4.04−2.06*log(a)
63.80−21.3a
142705
log(N)=−3.94−2.03*log(a)
63.80−21.4a
142703
log(N)=−3.99−2.05*log(a)
63.80−21.5a
142688
log(N)=−4.14−2.09*log(a)
63.80−21.6a
142654
log(N)=−4.40−2.17*log(a)
63.80−21.7a
142585
log(N)=−4.29−2.12*log(a)
63.80−21.8a
142573
log(N)=−4.25−2.11*log(a)
63.80−21.9a
142555
log(N)=−3.88−1.99*log(a)

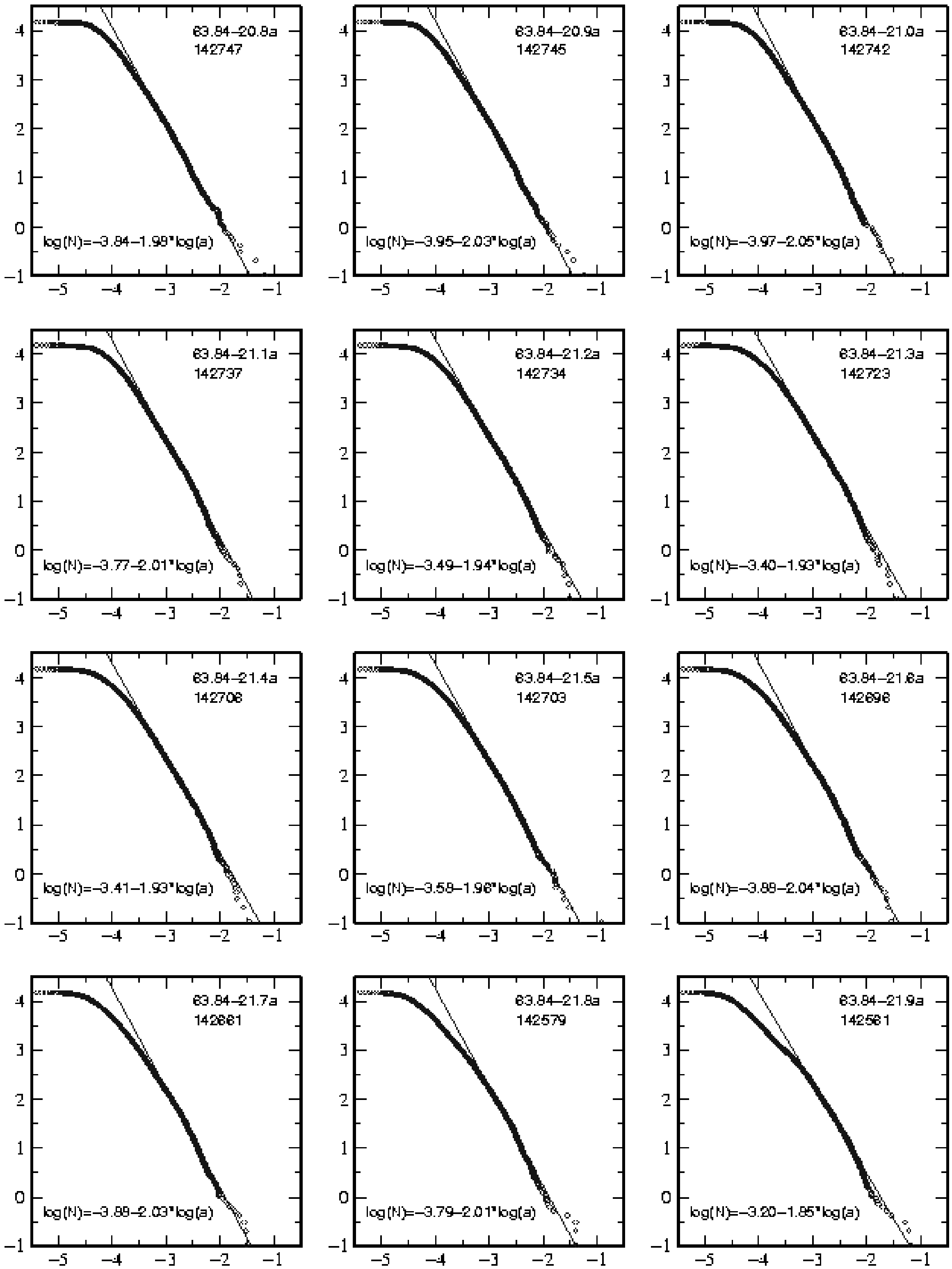
63.84–20.8a
142747
log(N)=–3.84–1.98*log(a)
63.84–20.9a
142745
log(N)=–3.95–2.03*log(a)
63.84–21.0a
142742
log(N)=–3.97–2.05*log(a)
63.84–21.1a
142737
log(N)=–3.77–2.01*log(a)
63.84–21.2a
142734
log(N)=–3.49–1.94*log(a)
63.84–21.3a
142723
log(N)=–3.40–1.93*log(a)
63.84–21.4a
142708
log(N)=–3.41–1.93*log(a)
63.84–21.5a
142703
log(N)=–3.58–1.96*log(a)
63.84–21.6a
142696
log(N)=–3.88–2.04*log(a)
63.84–21.7a
142661
log(N)=–3.88–2.03*log(a)
63.84–21.8a
142579
log(N)=–3.79–2.01*log(a)
63.84–21.9a
142561
log(N)=–3.20–1.85*log(a)

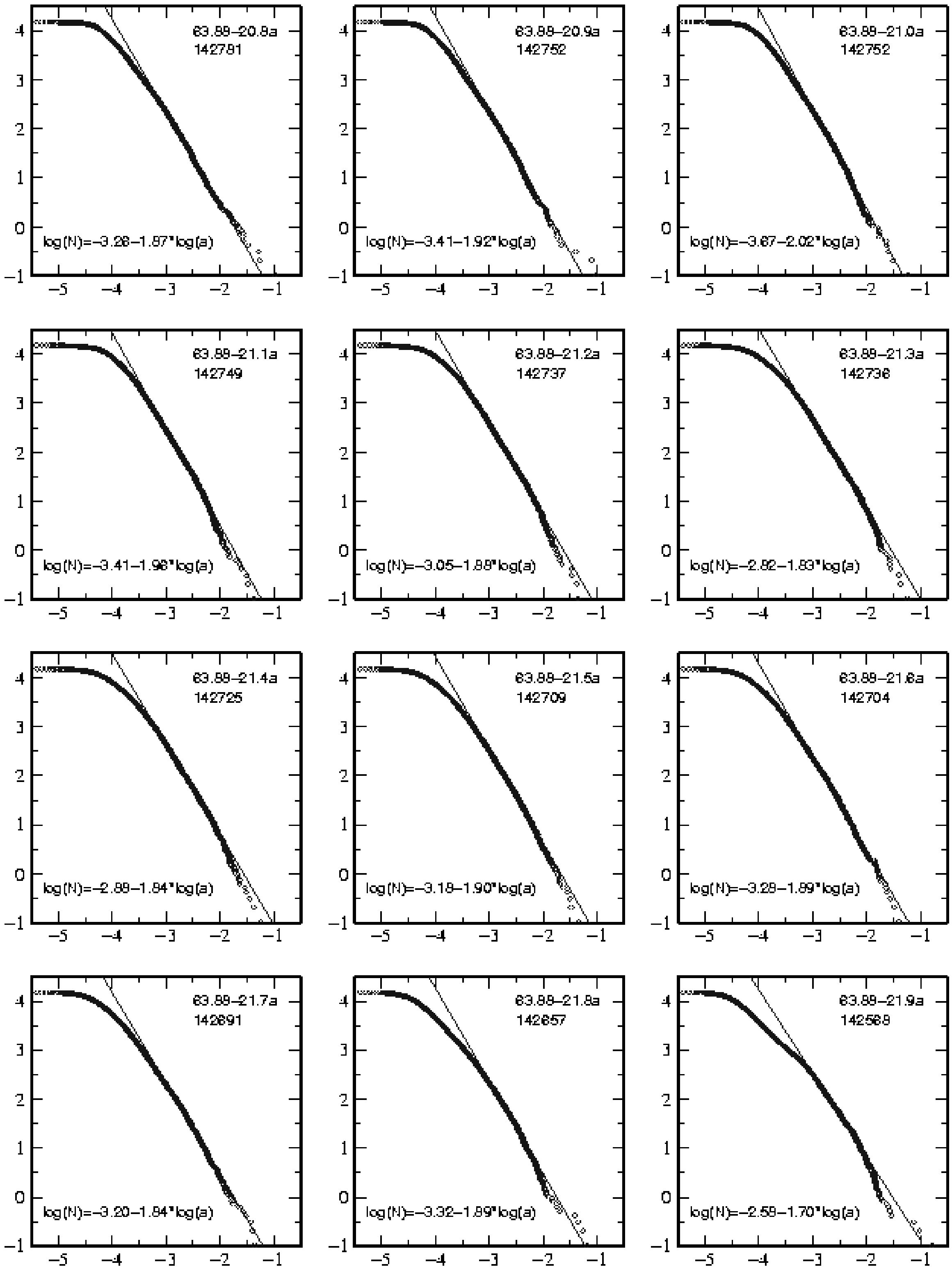
63.88–20.8a
142781
log(N)=–3.28–1.87*log(a)
63.88–20.9a
142752
log(N)=–3.41–1.92*log(a)
63.88–21.0a
142752
log(N)=–3.67–2.02*log(a)
63.88–21.1a
142749
log(N)=–3.41–1.98*log(a)
63.88–21.2a
142737
log(N)=–3.05–1.88*log(a)
63.88–21.3a
142738
log(N)=–2.82–1.83*log(a)
63.88–21.4a
142725
log(N)=–2.88–1.84*log(a)
63.88–21.5a
142709
log(N)=–3.18–1.90*log(a)
63.88–21.6a
142704
log(N)=–3.28–1.89*log(a)
63.88–21.7a
142691
log(N)=–3.20–1.84*log(a)
63.88–21.8a
142657
log(N)=–3.32–1.89*log(a)
63.88–21.9a
142588
log(N)=–2.58–1.70*log(a)

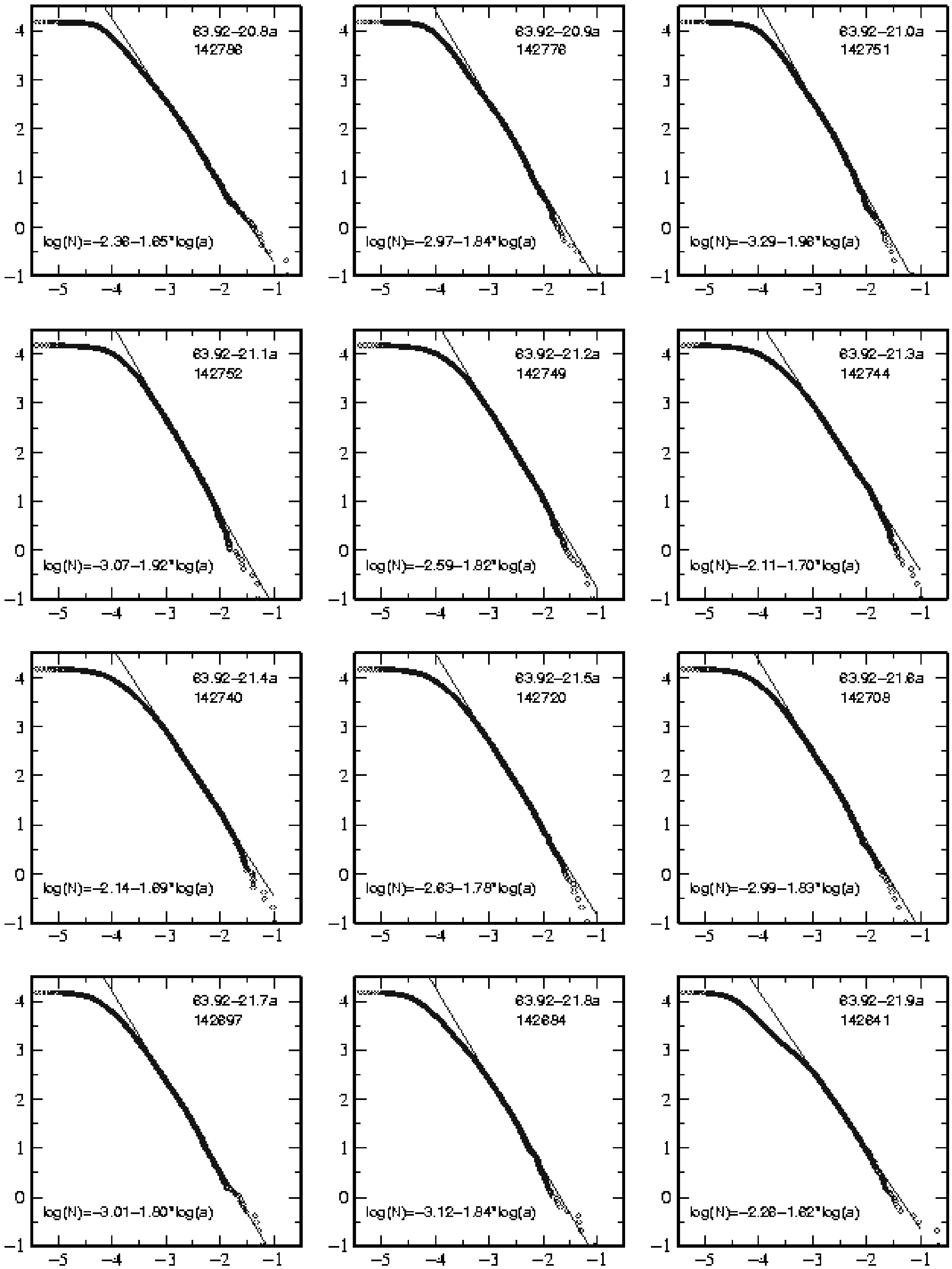
63.92−20.8a
142786
log(N)=−2.36−1.65*log(a)
63.92−20.9a
142776
log(N)=−2.97−1.84*log(a)
63.92−21.0a
142751
log(N)=−3.29−1.96*log(a)
63.92−21.1a
142752
log(N)=−3.07−1.92*log(a)
63.92−21.2a
142749
log(N)=−2.59−1.82*log(a)
63.92−21.3a
142744
log(N)=−2.11−1.70*log(a)
63.92−21.4a
142740
log(N)=−2.14−1.69*log(a)
63.92−21.5a
142720
log(N)=−2.63−1.76*log(a)
63.92−21.6a
142708
log(N)=−2.99−1.83*log(a)
63.92−21.7a
142697
log(N)=−3.01−1.80*log(a)
63.92−21.8a
142684
log(N)=−3.12−1.84*log(a)
63.92−21.9a
142641
log(N)=−2.26−1.62*log(a)

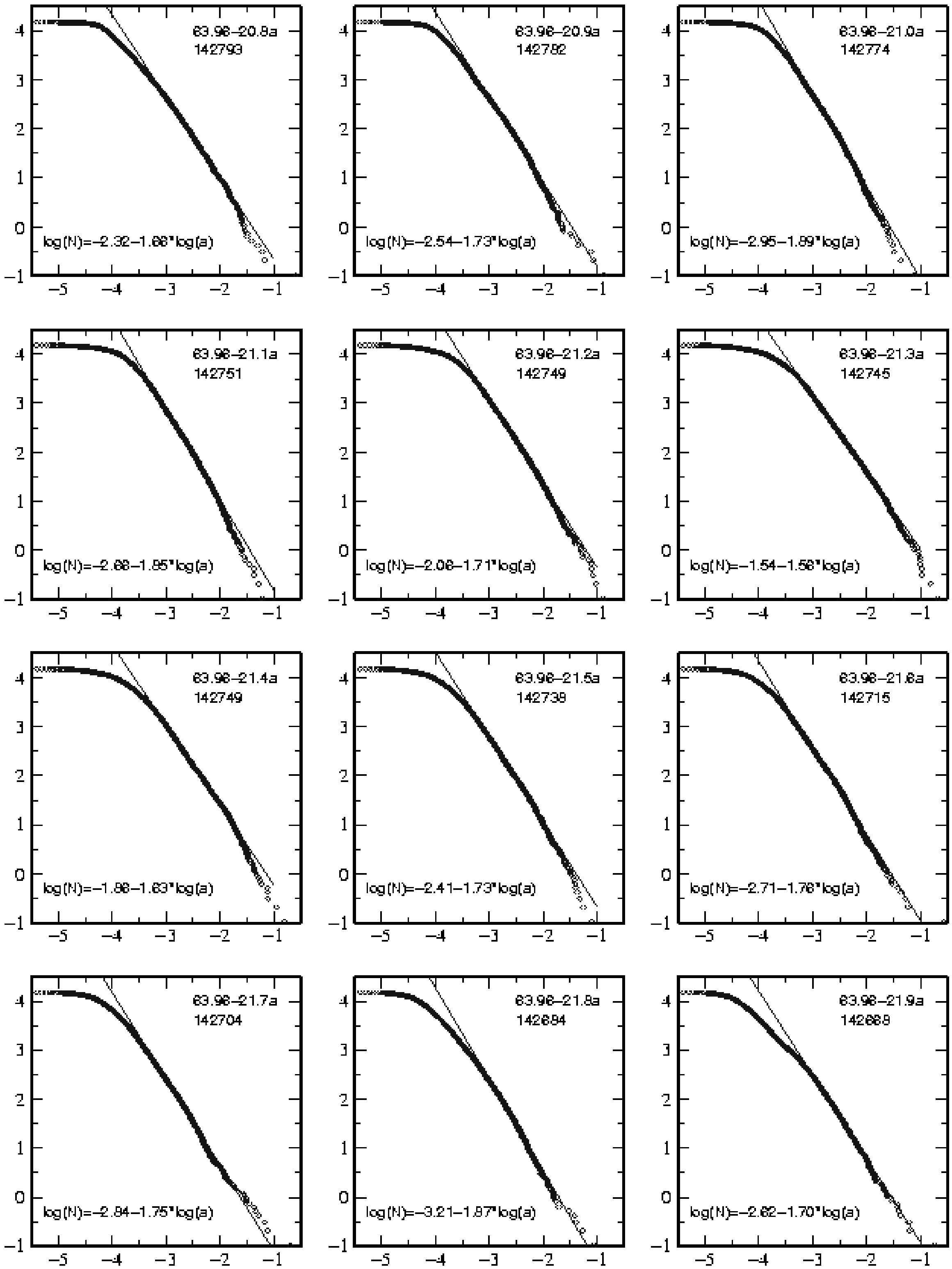
63.96-20.8a
142793
log(N)=-2.32-1.88*log(a)
63.96-20.9a
142782
log(N)=-2.54-1.73*log(a)
63.96-21.0a
142774
log(N)=-2.95-1.89*log(a)
63.96-21.1a
142751
log(N)=-2.68-1.85*log(a)
63.96-21.2a
142749
log(N)=-2.06-1.71*log(a)
63.96-21.3a
142745
log(N)=-1.54-1.56*log(a)
63.96-21.4a
142749
log(N)=-1.88-1.63*log(a)
63.96-21.5a
142738
log(N)=-2.41-1.73*log(a)
63.96-21.6a
142715
log(N)=-2.71-1.78*log(a)
63.96-21.7a
142704
log(N)=-2.84-1.75*log(a)
63.96-21.8a
142684
log(N)=-3.21-1.87*log(a)
63.96-21.9a
142688
log(N)=-2.82-1.70*log(a)

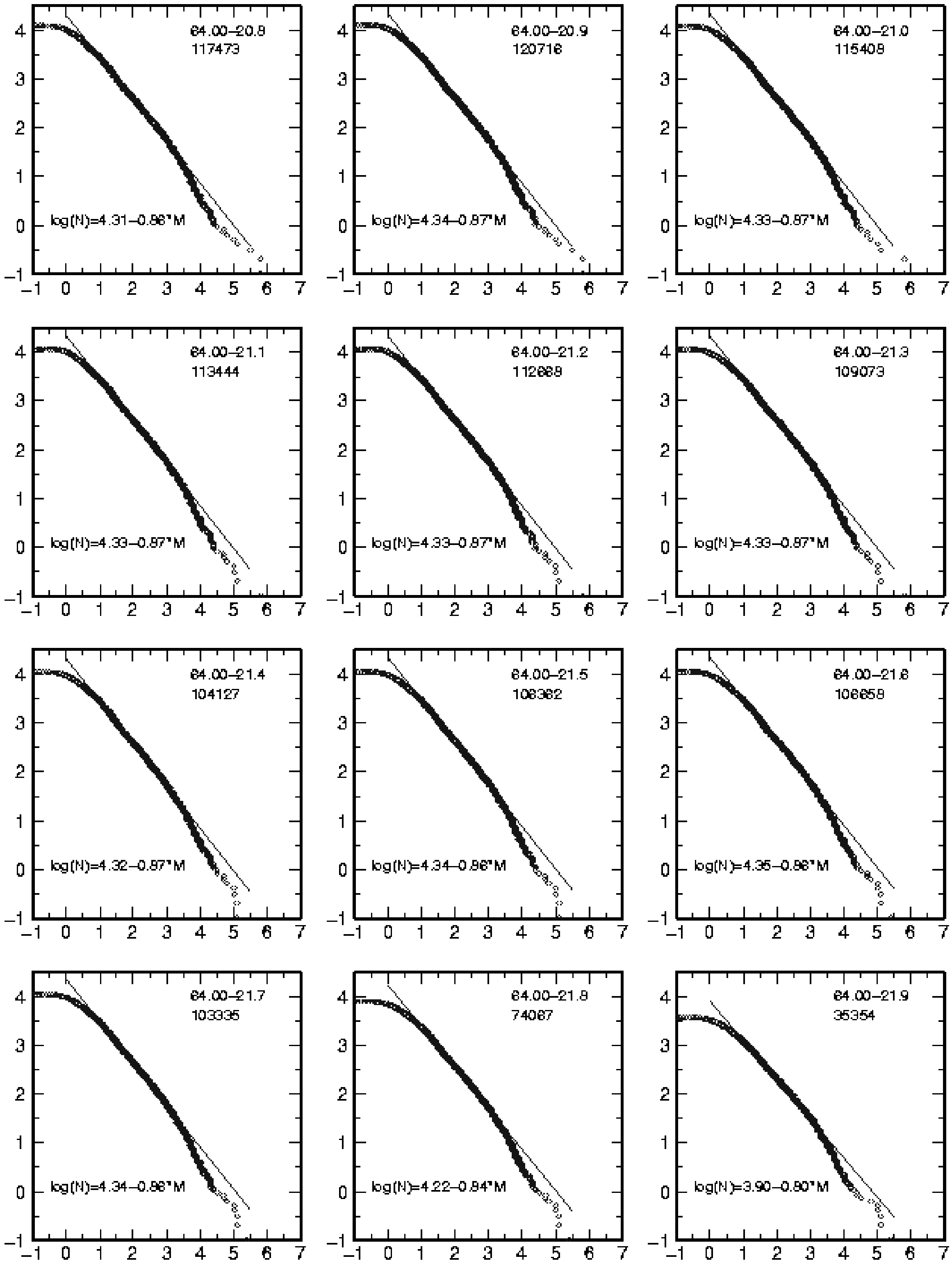
64.00–20.8
117473
log(N)=4.31–0.86*M
64.00–20.9
120716
log(N)=4.34–0.87*M
64.00–21.0
115408
log(N)=4.33–0.87*M
64.00–21.1
113444
log(N)=4.33–0.87*M
64.00–21.2
112688
log(N)=4.33–0.87*M
64.00–21.3
109073
log(N)=4.33–0.87*M
64.00–21.4
104127
log(N)=4.32–0.87*M
64.00–21.5
108382
log(N)=4.34–0.86*M
64.00–21.6
106658
log(N)=4.35–0.86*M
64.00–21.7
103335
log(N)=4.34–0.86*M
64.00–21.8
74087
log(N)=4.22–0.84*M
64.00–21.9
35354
log(N)=3.90–0.80*M

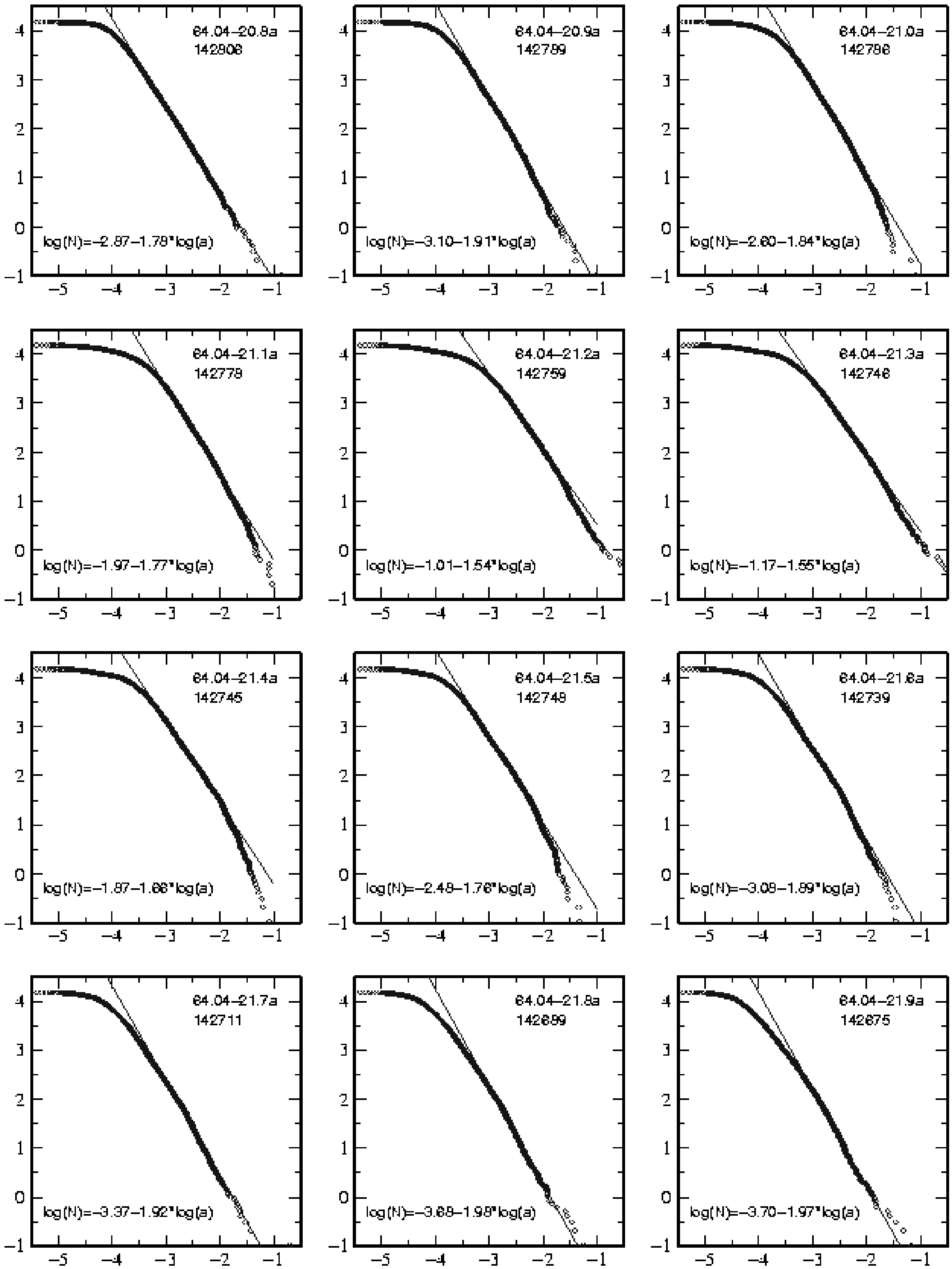

64.04–20.8a
142806
log(N)=–2.87–1.78*log(a)
64.04–20.9a
142799
log(N)=–3.10–1.91*log(a)
64.04–21.0a
142786
log(N)=–2.60–1.84*log(a)
64.04–21.1a
142778
log(N)=–1.97–1.77*log(a)
64.04–21.2a
142759
log(N)=–1.01–1.54*log(a)
64.04–21.3a
142746
log(N)=–1.17–1.55*log(a)
64.04–21.4a
142745
log(N)=–1.87–1.86*log(a)
64.04–21.5a
142748
log(N)=–2.48–1.76*log(a)
64.04–21.6a
142739
log(N)=–3.08–1.89*log(a)
64.04–21.7a
142711
log(N)=–3.37–1.92*log(a)
64.04–21.8a
142689
log(N)=–3.68–1.98*log(a)
64.04–21.9a
142675
log(N)=–3.70–1.97*log(a)

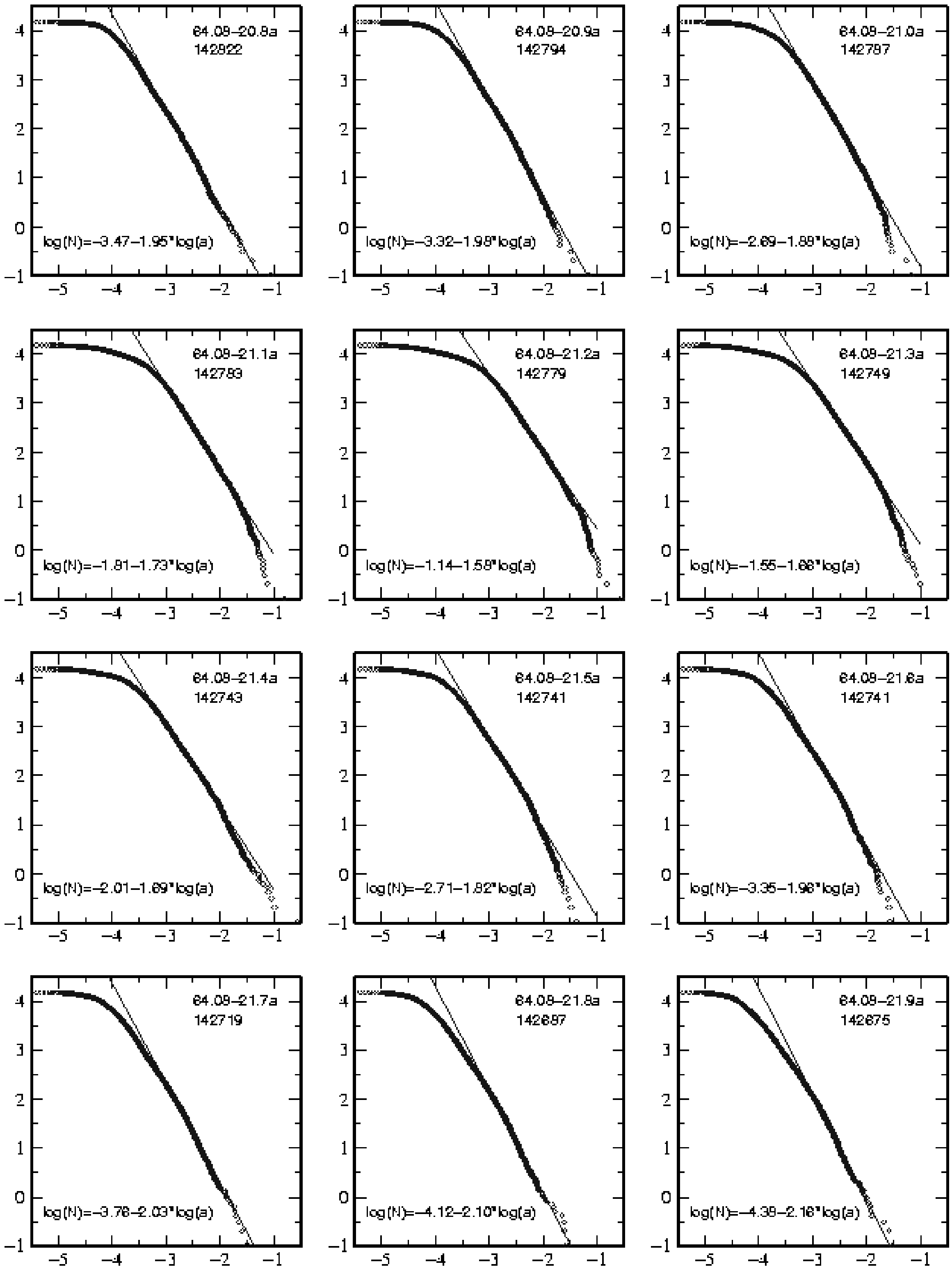
64.08–20.8a
142822
log(N)=–3.47–1.95*log(a)
64.08–20.9a
142794
log(N)=–3.32–1.98*log(a)
64.08–21.0a
142787
log(N)=–2.69–1.88*log(a)
64.08–21.1a
142783
log(N)=–1.81–1.73*log(a)
64.08–21.2a
142779
log(N)=–1.14–1.58*log(a)
64.08–21.3a
142749
log(N)=–1.55–1.68*log(a)
64.08–21.4a
142743
log(N)=–2.01–1.69*log(a)
64.08–21.5a
142741
log(N)=–2.71–1.82*log(a)
64.08–21.6a
142741
log(N)=–3.35–1.98*log(a)
64.08–21.7a
142719
log(N)=–3.78–2.03*log(a)
64.08–21.8a
142687
log(N)=–4.12–2.10*log(a)
64.08–21.9a
142675
log(N)=–4.38–2.16*log(a)

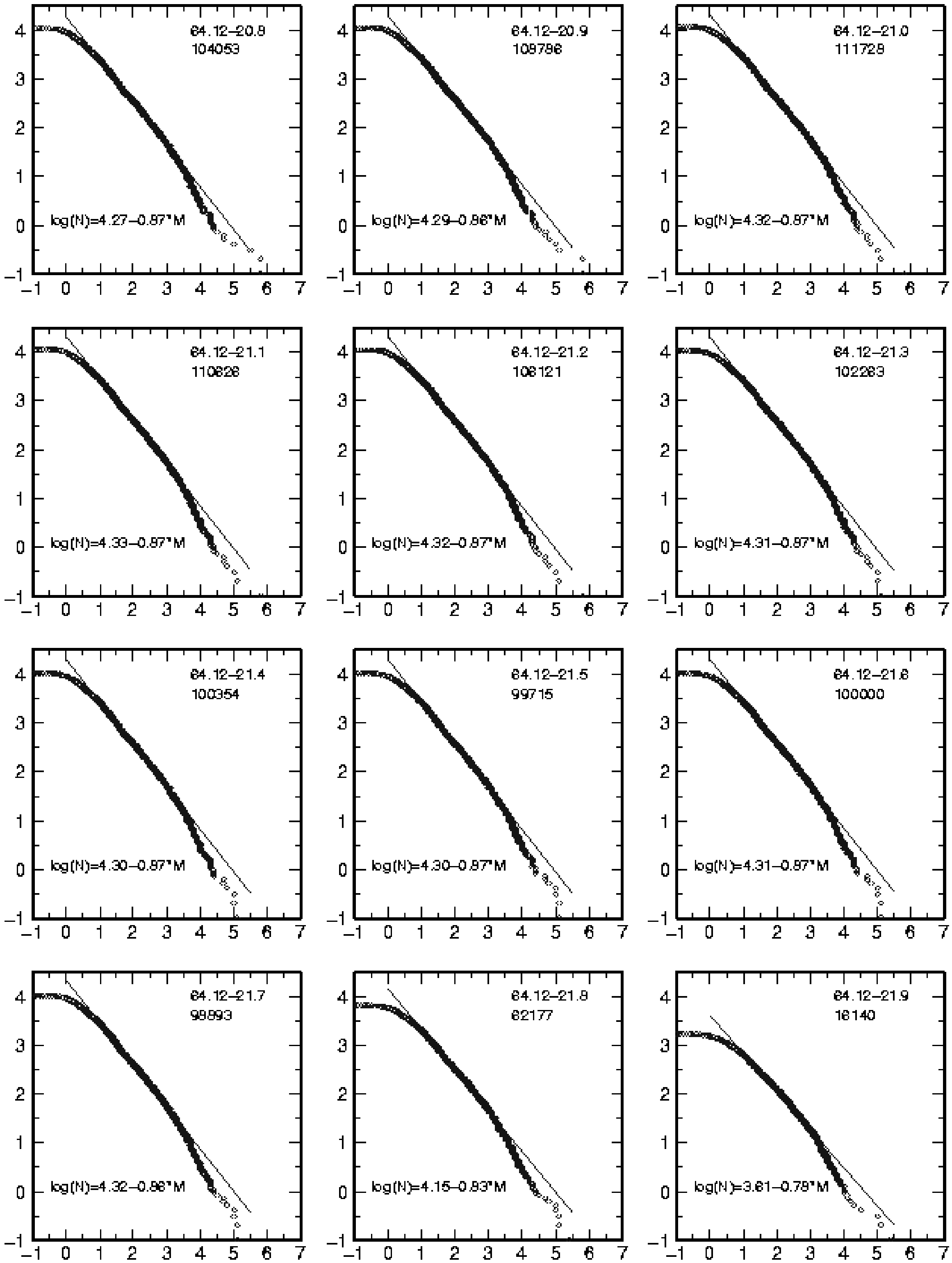
64.12−20.8
104053
log(N)=4.27−0.87*M
64.12−20.9
109786
log(N)=4.29−0.86*M
64.12−21.0
111728
log(N)=4.32−0.87*M
64.12−21.1
110828
log(N)=4.33−0.87*M
64.12−21.2
108121
log(N)=4.32−0.87*M
64.12−21.3
102283
log(N)=4.31−0.87*M
64.12−21.4
100354
log(N)=4.30−0.87*M
64.12−21.5
99715
log(N)=4.30−0.87*M
64.12−21.6
100000
log(N)=4.31−0.87*M
64.12−21.7
98893
log(N)=4.32−0.86*M
64.12−21.8
62177
log(N)=4.15−0.83*M
64.12−21.9
16140
log(N)=3.61−0.78*M

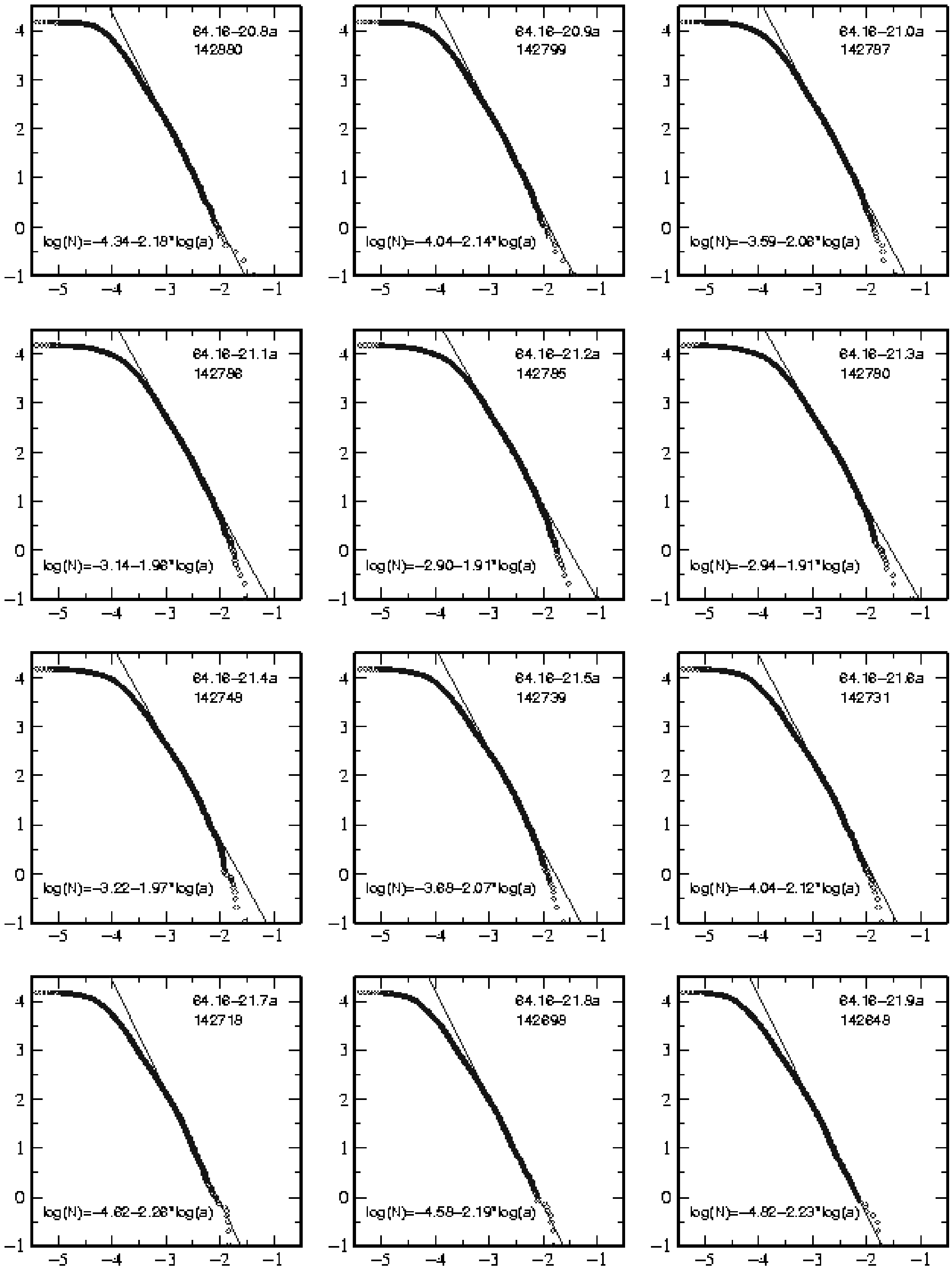
64.16–20.8a
142880
log(N)=–4.34–2.18*log(a)
64.16–20.9a
142799
log(N)=–4.04–2.14*log(a)
64.16–21.0a
142787
log(N)=–3.59–2.08*log(a)
64.16–21.1a
142786
log(N)=–3.14–1.98*log(a)
64.16–21.2a
142785
log(N)=–2.90–1.91*log(a)
64.16–21.3a
142780
log(N)=–2.94–1.91*log(a)
64.16–21.4a
142748
log(N)=–3.22–1.97*log(a)
64.16–21.5a
142739
log(N)=–3.68–2.07*log(a)
64.16–21.6a
142731
log(N)=–4.04–2.12*log(a)
64.16–21.7a
142718
log(N)=–4.62–2.26*log(a)
64.16–21.8a
142698
log(N)=–4.58–2.19*log(a)
64.16–21.9a
142648
log(N)=–4.82–2.23*log(a)

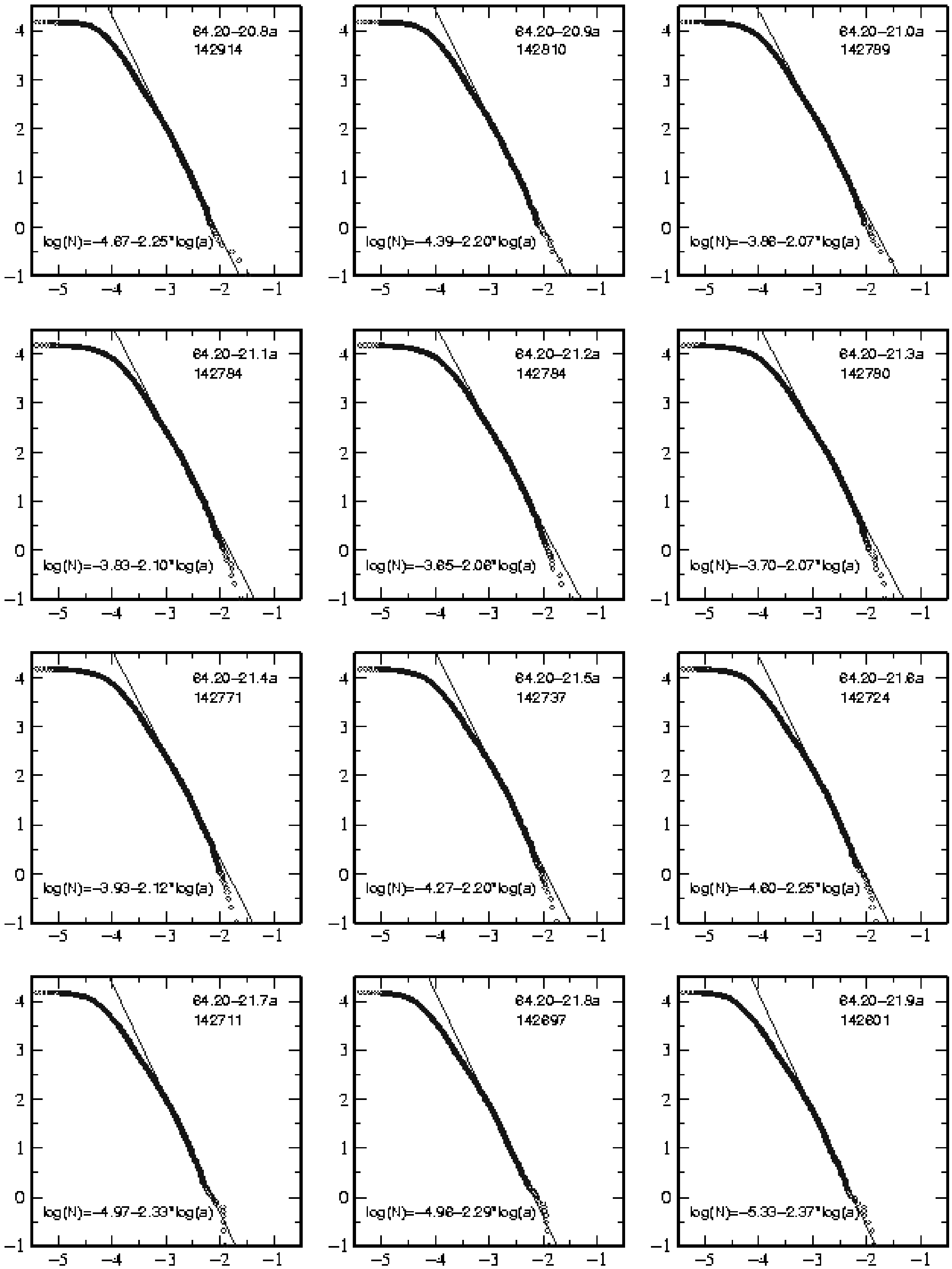
64.20-20.8a
142914
log(N)=-4.67-2.25*log(a)
64.20-20.9a
142810
log(N)=-4.39-2.20*log(a)
64.20-21.0a
142799
log(N)=-3.86-2.07*log(a)
64.20-21.1a
142784
log(N)=-3.83-2.10*log(a)
64.20-21.2a
142784
log(N)=-3.65-2.06*log(a)
64.20-21.3a
142780
log(N)=-3.70-2.07*log(a)
64.20-21.4a
142771
log(N)=-3.93-2.12*log(a)
64.20-21.5a
142737
log(N)=-4.27-2.20*log(a)
64.20-21.6a
142724
log(N)=-4.60-2.25*log(a)
64.20-21.7a
142711
log(N)=-4.97-2.33*log(a)
64.20-21.8a
142697
log(N)=-4.96-2.29*log(a)
64.20-21.9a
142601
log(N)=-5.33-2.37*log(a)

Appendix C

Hazard maps of the Hengill area showing horizontal acceleration to be reached or exceeded in a period of 100, 457, 2500 and 10000 years.

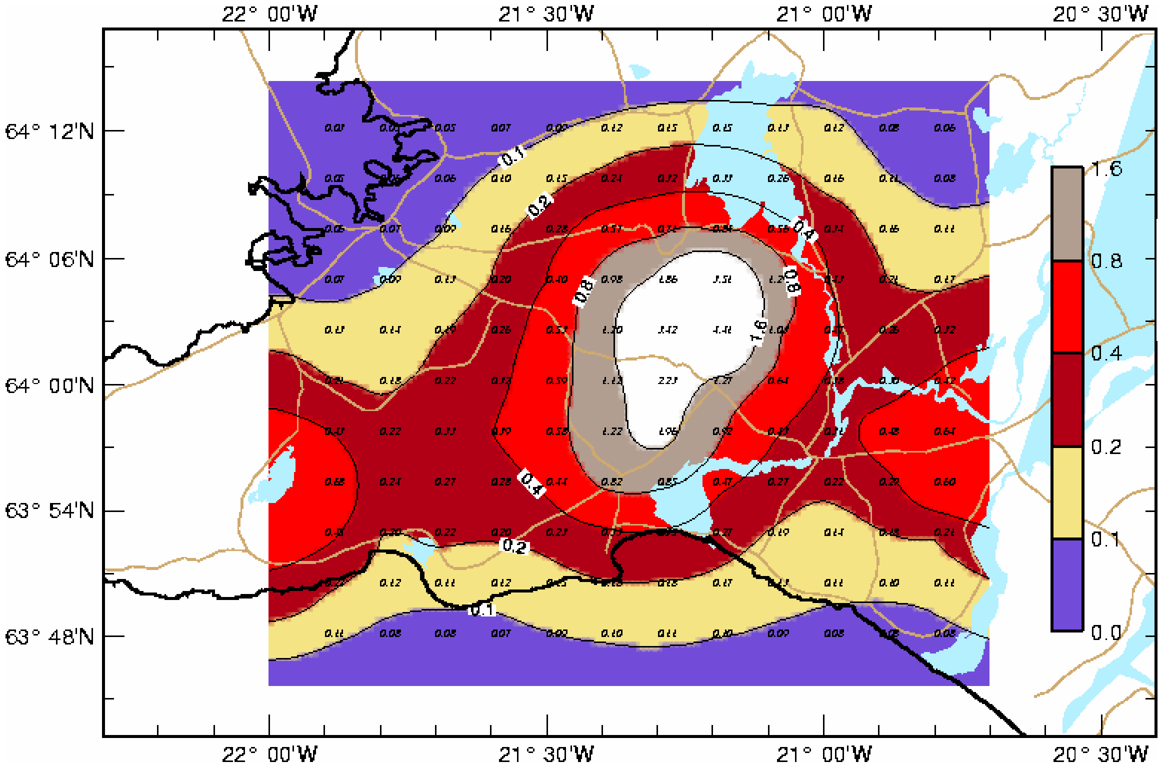

100 years

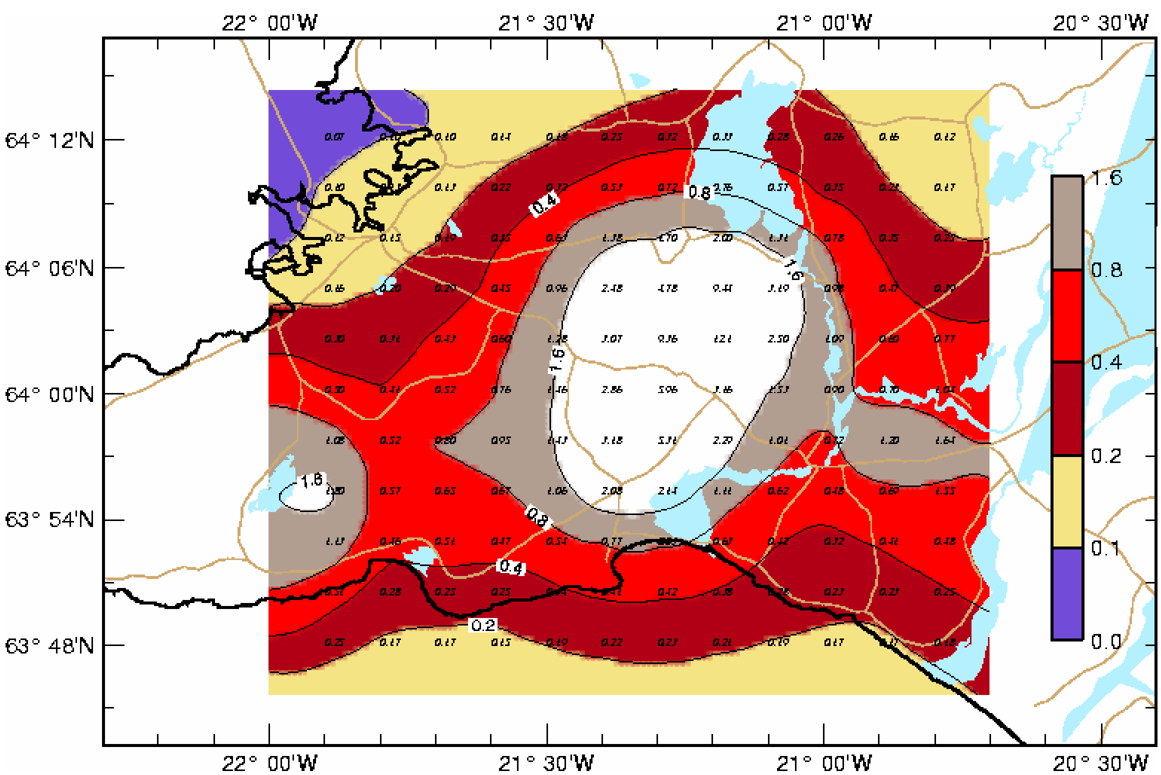

457 years

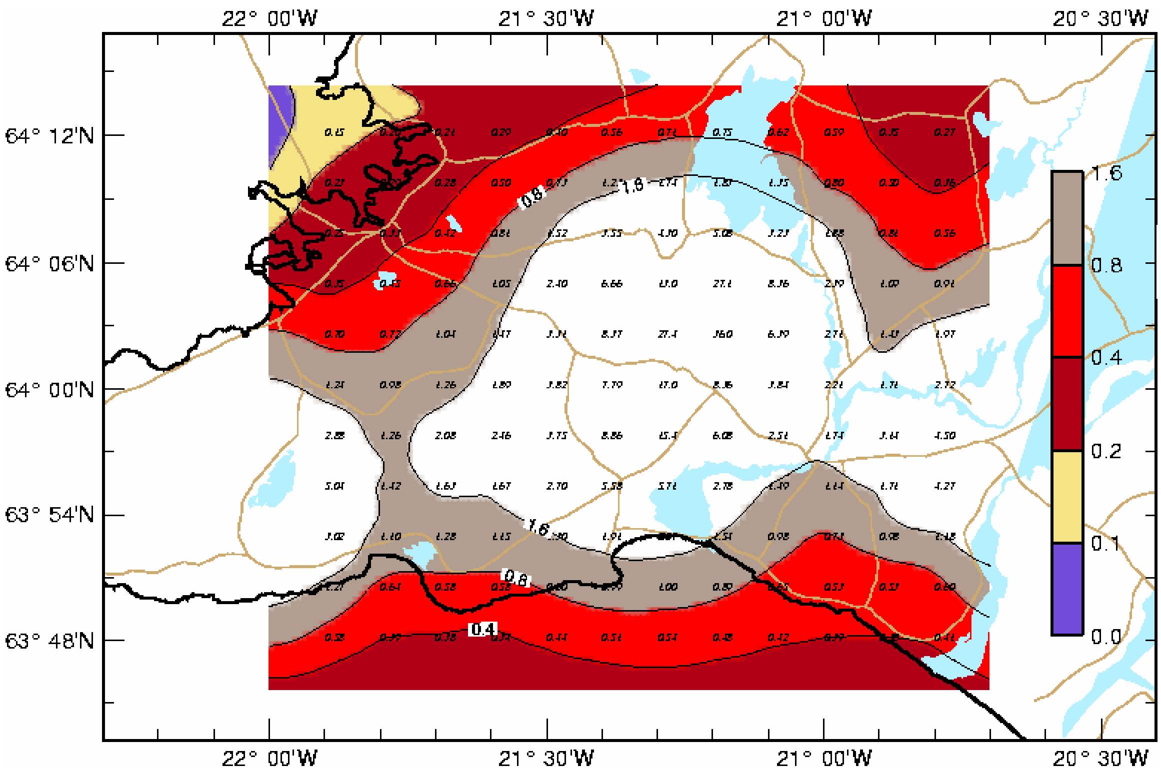

2500 years

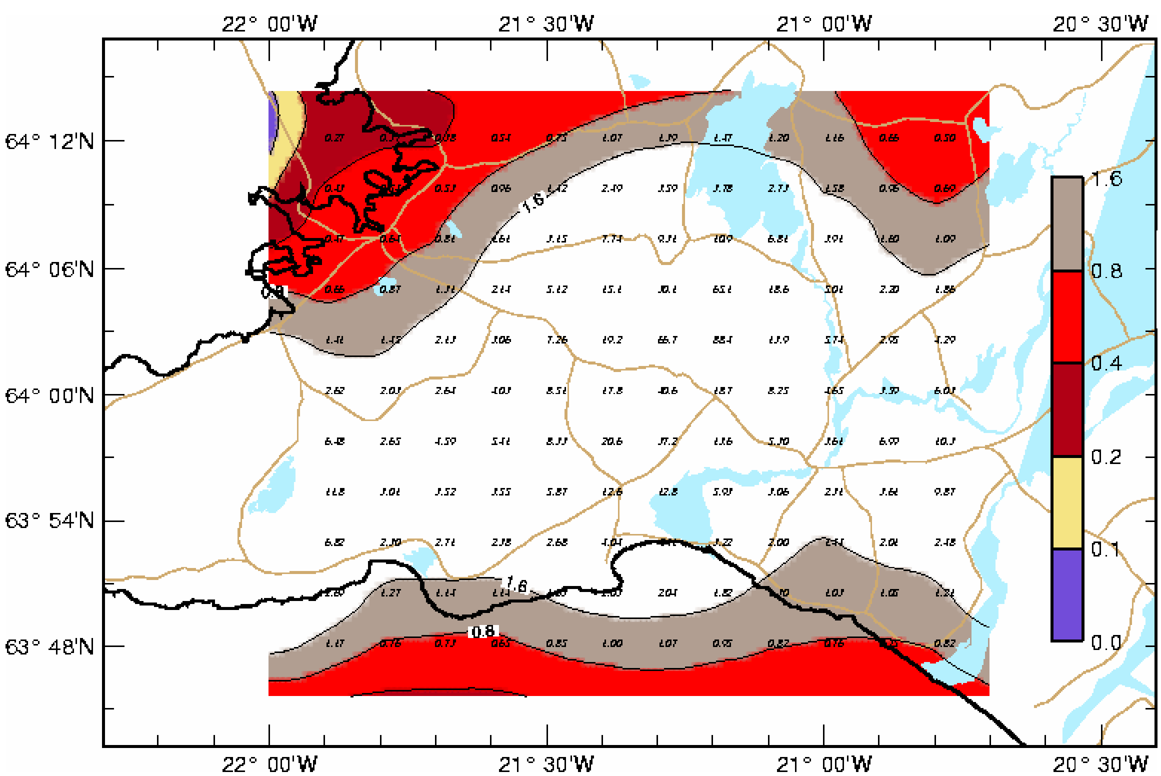

10000 years